arXiv:1501.00800v3 [cond-mat.str-el] 24 Mar 2015

Two-particle irreducible functional renormalization group schemes—a comparative study

J.F. Rentrop, S.G. Jakobs and V. Meden

Institut für Theorie der Statistischen Physik, RWTH Aachen University and
JARA - Fundamentals of Future Information Technology, 52062 Aachen,
Germany

E-mail: `jan.rentrop@rwth-aachen.de`

Abstract.
We derive functional renormalization group schemes for Fermi systems which are based on the two-particle irreducible approach to the quantum many-body problem. In a first step, the cutoff is introduced in the non-interacting propagator as it is commonly done in functional renormalization group based on one-particle irreducible vertex functions. The most natural truncation of the resulting infinite hierarchy of flow equations is shown to be fully equivalent to self-consistent perturbation theory. An earlier suggested alternative truncation strategy is considered as well. In a second step, the cutoff is introduced in the two-particle interaction. Again two truncation procedures are investigated, one of which was derived before. In the latter, the mean-field solution of the many-body problem is considered as the starting point of the renormalization group flow. We compare the performance and the required numerical resources for solving the coupled flow equations for all the approximate schemes by applying them to the problem of the quantum anharmonic oscillator. In a functional integral representation, this model has a formal similarity to the quantum many-body problem. The perspectives for applying the derived two-particle irreducible functional renormalization group approaches to zero- and one-dimensional systems of correlated fermions are discussed.

1. Introduction

Over the past years the functional renormalization group (fRG) was established as a versatile tool to study low-dimensional interacting Fermi systems [1, 2]. The variant almost exclusively used up to now is based on the generating functional for the one-particle irreducible (1PI) vertex functions. In this approach, one derives an exact infinite hierarchy of coupled differential flow equations for the 1PI vertex functions (self-energy and effective n-particle interactions), where the derivative is taken with respect to a flow parameter. Prior to practical calculations for any fermionic many-body model, a truncation of this set of coupled flow equations is required. Most truncation schemes were guided by perturbation theory in the flowing two-particle interaction rendering 1PI fRG a non-perturbative approximate method which is controlled for small to intermediate interactions. It is one of the assets of fRG based approximation schemes that they are unbiased in the sense that barely any a posteriori knowledge of the physics of the problem at hand must be used when setting them up. This e.g. allows for a faithful analysis of the interplay of distinct emergent quantum many-body phenomena.

The 1PI fRG was used to investigate the competing ordering tendencies (e.g. magnetism and unconventional superconductivity) in the two-dimensional Hubbard model and variants of the latter [1, 3], to study the spectral and transport properties of inhomogeneous one-dimensional lattice models (quantum wires) falling into the Luttinger liquid universality class [1], as well as of quantum impurity (quantum dot) models [1]. Compared to other RG approaches, fRG has the distinct advantage that it can directly be applied to microscopic lattice models and not only to low-energy effective field theories. This way, high-energy features and complex crossover behavior are captured.

For problems of interest in which plain perturbation theory in the two-particle interaction of characteristic amplitude U is divergent in the infrared limit (e.g. in two-dimensional models or in translationally invariant Luttinger liquids), the flow parameter must be introduced such that it has infrared regularizing properties; it acts as a low-energy cutoff [1]. In other systems, low-order perturbation theory is regular but, due to logarithmic terms with prefactor U^n, $n \in \mathbb{N}$, restricted to parameter regimes of infinitesimal extend. Then, 1PI fRG can be used to resum the logarithms generically leading to power-law behavior with U-dependent exponents [1]. In both cases, characteristics are utilized which are commonly associated to RG methods, e.g. the successive inclusion of energy scales from high to low and the resummation of logarithmic terms. However, 1PI fRG was also used for problems in which perturbation theory is regular and not plagued by logarithms. For such, fRG should be viewed as a “renormalization group enhanced perturbation theory” in which certain types of diagrams are resummed [1, 4, 5, 6]. It is then possible to employ other flow parameter schemes than the introduction of an infrared cutoff. One can e.g. think of successively turning on the strength of the two-particle interaction during the flow (see e.g. Ref. [7]).

Recent attempts to abandon the realm of small to intermediate interactions within fRG include to set up 1PI schemes in which certain aspects of the interaction are already included in the initial point of the RG flow [8, 9, 10]; e.g. the idea of taking dynamical mean-field theory containing all the local correlations as the starting point of the fRG flow was put forward [9]. In another attempt for a certain quantum impurity model, namely the single-impurity Anderson model, lots of a posteriori knowledge of the physics was built into the fRG procedure [11]. In the latter case, however, one gives up the strength of fRG of being unbiased. The 1PI fRG was recently extended to study quantum wires as well as quantum dots in non-equilibrium. The driven non-equilibrium steady state [12, 13, 14, 15] as well as the non-equilibrium time evolution [16] were investigated.

Despite its successes, present day 1PI fRG suffers from several shortcomings. For general two-dimensional models, it still constitutes a challenge to formulate an unbiased purely fermionic scheme which allows to extend the flow into phases with spontaneously broken symmetry [1]. Phase transitions are driven by composite fields and not the bare fermions. Crudely speaking, these composite degrees of freedom are not properly dealt with in the standard implementation of 1PI fRG. As a consequence, the RG flow diverges at a certain cutoff scale and has to be stopped. Therefore, only ordering tendencies can be read off but one cannot compute observables of the cutoff-free problem in the symmetry broken state. In recently developed novel schemes the flow is initialized including a small selected symmetry breaking term. In the parts of the parameter space in which the corresponding instability dominates, the flow is regularized and the cutoff can be removed allowing to investigate the symmetry broken phase [17, 18, 19, 20, 21]. Another way out is to introduce the bosonic composite degrees of freedom during the RG flow by partial "bosonization" [2, 22, 23, 24, 25, 26, 27], however, again to the price of giving up treating all instabilities on equal footing.

For zero-dimensional quantum impurity models, the above mentioned "flow to strong coupling" is not an issue and the truncated set of 1PI fRG flow equations can be integrated down to vanishing cutoff. From the resulting expressions for the vertex functions, approximate results for observables of interest such as the ground state energy or the single-particle spectral function of the cutoff-free model can be computed. However, case studies revealed that going to higher orders in the truncation does not necessarily lead to the hoped for improvement of the results beyond the limit of weak interactions (for which the results systematically improve). E.g. for the single-impurity Anderson model, the local spin susceptibility shows Kondo physics in first order truncation [5] but loses this property in second order [4, 6]. Similarly, for the interacting resonant level model, expected power-law behavior of observables confirmed in first order truncation is lost in second order [15].

A general drawback of the 1PI fRG for practical computations is that it is computationally costly to systematically include frequency dependence. This restricts the access to dynamical observables. A frequency dependence of the self-energy is only generated if the dependence of the two-particle vertex on its three independent frequencies (for a time translational invariant model) is kept [1]. This leads to an excessive growth of the number of equations to be considered.‡ Therefore, it was only for zero-dimensional quantum dot models with a few interacting degrees of freedom [4, 6] or toy models such as the quantum harmonic oscillator with quartic anharmonicity [4] that frequency dependence up to second order could be included completely. This e.g. prevented the study of bulk Luttinger liquid physics in one-dimensional models of interacting electrons. Schemes to include a frequency dependent self-energy for two-dimensional systems were put forward in Refs. [28, 29, 19].

Finally, it remains a challenge to fulfill Ward identities in truncated 1PI fRG approaches beyond the order in which the considered set of flow equations contains

‡ For an approximate treatment of the frequency dependence, see Refs. [4, 6, 14].

all diagrams of plain perturbation theory [30, 31, 11]. Therefore, the relation between approximate 1PI fRG schemes and so-called conserving approximations [32, 33] remains elusive.§

To circumvent the first mentioned drawback of 1PI fRG for problems of two-dimensional fermions, it was suggested in Refs. [35, 36] to set up fRG schemes based on the two-particle irreducible (2PI) approach to quantum many-body physics [32, 33]. This would allow to better incorporate the composite degrees of freedom. Such a procedure was earlier hinted at in Ref. [37]. However, recent results obtained by dynamical mean-field theory for models with phase transitions [38, 39] reveal unforeseen divergencies in the 2PI two-particle vertex. These might lead to obstacles for a 2PI fRG treatment of two-dimensional models.

We are primarily interested in interacting quantum dots and wires and here study 2PI fRG approaches to investigate their potential to overcome the second and third problem of 1PI fRG. Furthermore, using the same 2PI framework for fRG schemes as in standard conserving approximations promises insights on the relation to these.

In a first step, we derive four pair-wise related but different 2PI based fRG schemes. Two of them were introduced earlier [35, 36]. For these, we suggest modifications and provide insights which were not emphasized so far. Furthermore, we allude to the relations between all the approximate approaches. Instead of studying a fermionic many-body problem, we then apply these methods in a comparative study to the problem of the quantum harmonic oscillator with quartic anharmonicity. In a functional integral representation of the partition function, the anharmonic oscillator has the same structure as the one of a fermionic many-body problem (although with real fields instead of Grassmann fields). The anharmonicity g corresponds to the amplitude of the two-particle interaction in a many-body problem. Considering this toy model, we thus reduce the numerical effort (due to the reduced number of degrees of freedom and the more rapid decay of propagators) without sacrificing the general structure of the equations to be solved. We emphasize that the formal complexity of the problem we study is comparable to that of the single-impurity Anderson model [4]. The anharmonic oscillator was earlier used to illustrate the fRG procedure and to test newly developed fRG schemes [4, 40, 41, 42, 43]. It has the additional advantage that numerically exact results for observables of interest can easily be obtained. By comparing exact results to our approximate ones for the dependence of the ground state energy and the position fluctuations $\langle x^2 \rangle$ on g as well as for the frequency dependence of the self-energy at fixed g, we obtain an impression of the approximation quality. The 2PI fRG results are in addition compared to the ones of 1PI fRG. We furthermore discuss the advantages and drawbacks of the different schemes in their application to fermionic many-body problems.

We briefly study another fRG scheme which is not based on a 2PI generating functional but on one which is two-particle point-irreducible (2PPI). The use of this was suggested [44, 45] for its relation to density functional theory and applied to the anharmonic oscillator in Ref. [46]. The results of the 2PPI approach to the anharmonic oscillator are compared to those of 2PI.

We identify two 2PI schemes in which a frequency dependent self-energy is generated consistently without having to deal with functions of three independent frequencies. Compared to the standard frequency dependent 1PI approach this considerably reduces the numerical effort. Nevertheless, the accuracy of these two

---

§ For recent considerations on the relation between fRG and Schwinger-Dyson equations, see Ref. [34].

2PI schemes for the anharmonic oscillator is satisfactory. For one of them, it is even slightly superior to 1PI fRG. It remains to be seen if the same holds for fermionic many-body systems. We furthermore prove that the most natural truncation of the 2PI flow equations with the flow parameter introduced via the free single-particle propagator exactly gives the well known self-consistent perturbation theory (conserving approximation), e.g. in lowest order the self-consistent Hartree-Fock approximation.

Our paper is organized as follows. In Sect. 2, we give the functional integral representation of the partition function of interest. The generating functionals of the 2PI formalism are introduced in Sect. 3. In Sect. 4, we present a first 2PI fRG approach which results from including the flow parameter in the free propagator C (as is mostly done in 1PI fRG); we coin it C-flow. The two approximation schemes resulting from C-flow as well as their application to the anharmonic oscillator are presented in subsections. As a sequel of Sect. 3, we present technical details of the pair propagator and the Bethe-Salpeter equation in Sect. 5 which are crucial for the second 2PI fRG approach, the so-called U-flow. In this approach, the flow parameter is introduced via the amplitude U of the two-particle interaction as described in Sect. 6. Again, subsections are devoted to two resulting approximation schemes. In one, the non-interacting problem is considered as the starting point of the RG flow; in the other, the flow is started from the mean-field solution of the problem at hand. The results of these schemes for the anharmonic oscillator are presented in another subsection. In Sect. 7, we give a brief account of the 2PPI fRG and discuss our results for the anharmonic oscillator. The results for the most successful approximate 2PI and 2PPI schemes are compared to the ones of 1PI in a concluding Sect. 8. It also contains a brief discussion of the perspectives of applying 2PI fRG to fermionic quantum many-body problems. In the Appendix, we give some details of our numerical implementation of the frequency dependence.

2. The fermionic many-body problem and the anharmonic oscillator

We are interested in a 2PI fRG approach to fermionic quantum many body problems. The starting point for the definition of suitable generating functionals is the grand canonical partition function of a system of interacting fermions written in coherent state functional integral representation [47],

$$Z = \operatorname{tr} e^{-\beta(H-\mu N)} = \int D[\psi] e^{-S[\psi]}, \tag{1}$$

where the action is

$$S[\psi] = -\frac{1}{2}\sum_{\alpha\alpha'} \psi_\alpha \left(C^{-1}\right)_{\alpha\alpha'} \psi_{\alpha'} + \frac{1}{4!}\sum_{\alpha_1\alpha_1'\alpha_2\alpha_2'} U_{\alpha_1\alpha_1'\alpha_2\alpha_2'}\psi_{\alpha_1}\psi_{\alpha_1'}\psi_{\alpha_2}\psi_{\alpha_2'}. \tag{2}$$

Following Refs. [35, 36], we use a fully antisymmetrized notation here. This is customary in 2PI approaches and allows to derive the Bethe-Salpeter equation in arbitrary channels, compare Sect. 5. The notation is based on indices $\alpha = (c, \tau, y)$ with charge index $c = \pm$, imaginary time τ and single-particle quantum number y. The fields $\psi_{-,\tau y} = \psi_y(\tau)$, $\psi_{+,\tau y} = \overline{\psi}_y(\tau)$ take Grassmann number values. The inverse free propagator is antisymmetric, $C^{-1}_{\alpha'\alpha} = -C^{-1}_{\alpha\alpha'}$, and satisfies

$$C^{-1}_{(+,\tau_1 y_1)(-,\tau_2 y_2)} = -\delta(\tau_1-\tau_2)(\partial_{\tau_2} + \epsilon_{y_1 y_2}), \tag{3}$$

where ϵ is the matrix of $(H_0 - \mu N)$ in the single-particle basis. Here, H_0 denotes the non-interacting part of the Hamiltonian H. The two-particle interaction vertex U is fully antisymmetric under permutation of its indices, $U_{\alpha_1\alpha_2\alpha_3\alpha_4} = (-1)^P U_{\alpha_{P1}\alpha_{P2}\alpha_{P3}\alpha_{P4}}$.

In the following, we study various 2PI fRG methods. Since the application of such schemes to many-body problems (like the Anderson impurity model) is involved, we here employ them to a simpler toy model in a first step. For that purpose, a "classical" choice [4, 41, 42, 43] is the quantum anharmonic oscillator with Hamiltonian

$$H = \frac{\hat{p}^2}{2} + V(\hat{x}) = \frac{\hat{p}^2}{2} + \frac{\omega_{\mathrm{G}}^2}{2}\hat{x}^2 + \frac{g}{4!}\hat{x}^4. \tag{4}$$

The position eigenstate path integral expression for its canonical partition function is

$$Z = \operatorname{tr} e^{-\beta H} = \int D[x] e^{-S[x]} \tag{5}$$

with real fields x, a suitably normalized measure $D[x]$, and the corresponding action (see e.g. Ref. [47])

$$S = \int_0^\beta d\tau \left\{ \frac{[\partial_\tau x(\tau)]^2}{2} + V\big(x(\tau)\big) \right\} = \int_0^\beta d\tau \left\{ \frac{1}{2} x(\tau) \left(\overleftarrow{\partial}_\tau \overrightarrow{\partial}_\tau + \omega_{\mathrm{G}}^2 \right) x(\tau) + \frac{g}{4!} \left[x(\tau)\right]^4 \right\}. \tag{6}$$

Here, $\overleftarrow{\partial}_\tau$ ($\overrightarrow{\partial}_\tau$) denotes a partial derivative that acts to the left (right). If we define the totally symmetric quantities

$$C^{-1}(\tau,\tau') = -\overleftarrow{\partial}_\tau \delta(\tau-\tau') \overrightarrow{\partial}_{\tau'} - \delta(\tau-\tau')\omega_{\mathrm{G}}^2, \tag{7}$$

$$U(\tau_1,\tau_1',\tau_2,\tau_2') = \delta(\tau_1'-\tau_1)\delta(\tau_2-\tau_1)\delta(\tau_2'-\tau_1)g, \tag{8}$$

and identify $\tau = \alpha$ as well as $x = \psi$, the action has formally the same structure as given in Eq. (2) for the many-body problem. Due to the missing charge and state indices, computations for the quantum anharmonic oscillator are analytically simpler and numerically faster than for actual many-body problems. Typical observables can even be computed numerically exact which allows to assess the quality of approximate methods. Of course, the results cannot be directly transferred to many-body problems, since the fields are of different nature (real fields vs. Grassmann ones) and the additional degrees of freedom in many-body problems often lead to much richer physics. Nevertheless, basic properties of different approximation procedures can be tested on the anharmonic oscillator.

The general derivations in the following sections hold for the fermionic many-body problem as well as for the anharmonic oscillator. Occasionally, the different commutation properties of Grassmann and real numbers lead to different sign prefactors. Then, $\zeta = -1$ applies to fermions and $\zeta = +1$ to the anharmonic oscillator.

3. Generating functionals in the 2PI formalism

In this section, we briefly recall some basic relations for the generating functionals in the 2PI formalism and introduce the corresponding notation. We start by defining the functional

$$Z[J] = e^{W[J]} = \int D[\psi] e^{-S[\psi] + \frac{1}{2}\sum_{\alpha\alpha'} \psi_\alpha J_{\alpha\alpha'} \psi_{\alpha'}}. \tag{9}$$

The external source J is coupled to two fields here (cf. Refs. [47, 48]), which is decisive to obtain 2PI quantities by the Legendre transformation given below. J is defined to have the same (anti-)symmetry as C^{-1}, that is $J_{\alpha'\alpha} = \zeta J_{\alpha\alpha'}$. The first functional derivative of $W[J]$ leads to the (time ordered) expectation value of $\psi_\alpha\psi_{\alpha'}$, that is to the propagator,

$$W^{(1)}_{\alpha\alpha'}[J] = \frac{\delta W[J]}{\delta J_{\alpha\alpha'}} = \langle\psi_\alpha\psi_{\alpha'}\rangle_J = -G_{\alpha\alpha'}[J]. \tag{10}$$

In the following, it turns out to be convenient to use a combined index $\gamma = (\alpha, \alpha')$. The higher derivatives

$$W^{(n)}_{\gamma_1\cdots\gamma_n} = \frac{\delta^n W}{\delta J_{\gamma_1}\ldots\delta J_{\gamma_n}} \tag{11}$$

are the $2n$-point Green functions that are connected if each pair (α_i, α'_i) is considered intrinsically connected. They obey the symmetry relations

$$W^{(n)}_{\gamma_1\cdots\gamma_n} = W^{(n)}_{\gamma_{P1}\cdots\gamma_{Pn}}, \qquad W^{(n)}_{(\alpha_1,\alpha'_1),\gamma_2\cdots\gamma_n} = \zeta W^{(n)}_{(\alpha'_1,\alpha_1),\gamma_2\cdots\gamma_n} \tag{12}$$

for arbitrary permutations P.

The Legendre transformation of $W[J]$ leads to a functional of the free variable G which is called 2PI effective action,

$$\Gamma[G] = \{-W[J] - J\cdot G\}|_{J[G]}\,. \tag{13}$$

Here we used a dot-product notation,

$$J\cdot G = \frac{1}{2}\sum_\gamma J_\gamma G_\gamma = \frac{1}{2}\sum_{\alpha\alpha'} J_{\alpha\alpha'}G_{\alpha\alpha'} = \frac{\zeta}{2}\operatorname{tr} JG = G\cdot J, \tag{14}$$

where the factor $\frac{1}{2}$ is related to the (anti-)symmetry of the factors under exchange of α and α'. As the quadratic part of the action is given by $(C^{-1}+J)\cdot(\psi\psi)$, it follows that $\Gamma[G] = \Gamma[G, C]$ depends explicitly on C, namely due to an addend $C^{-1}\cdot G = \frac{\zeta}{2}\operatorname{tr} C^{-1}G$. In the non-interacting case, one finds

$$W_0[J] = \ln[\det(-C^{-1} - J)]^{-\zeta/2} = -\frac{\zeta}{2}\operatorname{tr}\ln(-C^{-1} - J), \tag{15}$$

$$\Gamma_0[G] = -\frac{\zeta}{2}\big[\operatorname{tr}\ln(-G) - \operatorname{tr}(C^{-1}G - 1)\big]. \tag{16}$$

The Luttinger-Ward functional Φ is defined as

$$\Phi[G] = \Gamma[G] - \Gamma_0[G] \tag{17}$$

and does not depend on C. The first functional derivative of Γ and Φ is

$$\Gamma^{(1)}_\gamma[G] = \frac{\delta\Gamma[G]}{\delta G_\gamma} = -J_\gamma[G], \tag{18}$$

$$\Phi^{(1)}_\gamma[G] = \frac{\delta\Phi[G]}{\delta G_\gamma} = G^{-1}_\gamma - C^{-1}_\gamma - J_\gamma[G] = -\Sigma_\gamma[G], \tag{19}$$

where Σ denotes the self-energy. In the last step, we used that the effective free (i.e. non-interacting) propagator in the model with external sources is given by $(C^{-1}+J)^{-1}$. As $\Sigma[G]$ is the sum of all amputated one-particle 2PI diagrams with full propagator lines, it follows that $\Phi[G]$ is the sum of all vacuum 2PI diagrams (which are all 3PI) with full propagator lines. This expansion is shown in Fig. 1 and given by

$$\begin{aligned}\Phi[G] = {} & \frac{1}{8}\sum_{\gamma_1\gamma_2} U_{\gamma_1\gamma_2}G_{\gamma_1}G_{\gamma_2} \\ & -\frac{1}{48}\sum_{\gamma_1\gamma_2\gamma_3\gamma_4} U_{\alpha_1\alpha_2\alpha_3\alpha_4}U_{\alpha'_1\alpha'_2\alpha'_3\alpha'_4}G_{\gamma_1}G_{\gamma_2}G_{\gamma_3}G_{\gamma_4} + \mathcal{O}\left(U^3G^6\right).\end{aligned} \tag{20}$$

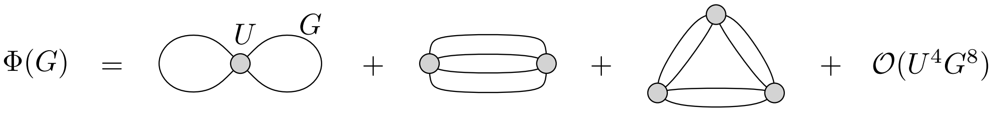

Figure 1. Diagrammatic expansion of the Luttinger-Ward functional $\Phi[G]$.

This was derived e.g. in Ref. [37] for fermions and holds as well for the anharmonic oscillator. The individual addends are proportional to U^nG^{2n}. In this expansion, it is apparent as well that Φ does not depend on C. The higher derivatives $\Gamma^{(n)} = \delta^n\Gamma/\delta G\ldots\delta G$ and $\Phi^{(n)} = \delta^n\Phi/\delta G\ldots\delta G$ satisfy symmetry relations that are analogous to Eq. (12).

Physical quantities are obtained at vanishing external source $J = 0$. We mark those quantities by overlining, hence $\overline{J} = 0, \overline{Z} = Z[\overline{J}], \overline{G} = G[\overline{J}]$, etc. For the Legendre transformed functions of the free variable G, the physical state is defined equivalently by $\Gamma^{(1)}[\overline{G}] = 0$ and we write $\overline{\Gamma} = \Gamma[\overline{G}], \overline{\Phi}^{(1)} = \Phi^{(1)}[\overline{G}]$ and so on. For systems with spontaneously broken symmetry there may be several physical states.

4. C-flow

4.1. Flow parameter, flow equations, initial conditions

In this section, we analyze 2PI fRG schemes where the flow parameter is introduced in the free propagator, $C \to C_\lambda$ (cf. Ref. [35]). This method will be referred to as "C-flow". As in 1PI fRG schemes [1], we choose the λ-dependence such that $C_{\lambda_\mathrm{i}} = 0$ at the beginning of the flow which ensures simple initial conditions for the flowing moments of Φ (see below). We enforce that at the end of the RG flow $C_{\lambda_\mathrm{f}} = C$ such that the cutoff-free system of interest is restored.

The λ-dependence of the free propagator C_λ makes the action and the functionals depend on λ: $S \to S_\lambda, Z \to Z_\lambda$, etc. From now on, we suppress the index λ most times to avoid overloading the notation. The flow of the functionals is given by

$$\dot{Z}[J] = \frac{\delta Z}{\delta J}\cdot \dot{C}^{-1}, \tag{21}$$

$$\dot{W}[J] = \frac{\dot{Z}}{Z} = W^{(1)}[J]\cdot \dot{C}^{-1}, \tag{22}$$

$$\dot{\Gamma}[G] = -\,\dot{W}\Big|_{J[G]} - \frac{\delta W}{\delta J}\cdot \dot{J} - \dot{J}\cdot G = -\,\dot{W}\Big|_{J[G]} = G\cdot \dot{C}^{-1}. \tag{23}$$

Here, the dot denotes the derivative with respect to λ, like $\dot{Z} = dZ_\lambda/d\lambda$ and $\dot{C}^{-1} = d(C_\lambda^{-1})/d\lambda$. We observe that $\dot{\Gamma}$ is independent of the interaction, $\dot{\Gamma} = \dot{\Gamma}_0$ (recall that G is the free variable of Γ and thus independent of the interaction). Consequently, the Luttinger-Ward functional $\Phi = \Gamma - \Gamma_0$ constitutes an invariant of the RG flow,

$$\dot{\Phi}[G] = 0. \tag{24}$$

This is expected since Φ does not depend on C which carries the flow parameter [cf. Eq. (20)]. The flow equations for the physical values of the moments of Φ are thus

$$\dot{\overline{\Phi}}{}^{(n)}_{\gamma_1\cdots\gamma_n} = \frac{d}{d\lambda}\Phi^{(n)}_{\gamma_1\ldots\gamma_n}[\overline{G}_\lambda] = \frac{1}{2}\sum_{\gamma}\overline{\Phi}^{(n+1)}_{\gamma_1\ldots\gamma_n\gamma}\dot{\overline{G}}_\gamma, \tag{25}$$

or briefly $\dot{\overline{\Phi}}^{(n)} = \overline{\Phi}^{(n+1)} \cdot \dot{\overline{G}}$ for $n = 0, 1, 2, \ldots$, which is an infinite coupled hierarchy comparable to those known from the 1PI fRG [1].

The propagator $\dot{\overline{G}}$ that enters the flow equations can be computed from $\overline{G} = (C^{-1} - \overline{\Sigma})^{-1}$,

$$\dot{\overline{G}} = -\overline{G} \left(\dot{C}^{-1} - \dot{\overline{\Sigma}} \right) \overline{G}, \tag{26}$$

a result that depends in turn on $\dot{\overline{\Sigma}} = -\dot{\overline{\Phi}}^{(1)}$. This leads to a self-consistent flow equation for the self-energy,

$$\dot{\overline{\Sigma}} = \overline{\Phi}^{(2)} \cdot \overline{G} \left(\dot{C}^{-1} - \dot{\overline{\Sigma}} \right) \overline{G}. \tag{27}$$

An alternative approach to computing $\dot{\overline{G}}$ is given by $\dot{\overline{G}} = -\overline{W}^{(2)} \cdot \dot{\Gamma}^{(1)}|_{\overline{G}} = -\overline{W}^{(2)} \cdot \dot{C}^{-1}$ which is derived in Sect. 6.1, compare Eq. (78). This, however, requires the solution of the Bethe-Salpeter equation (72) for $W^{(2)}$.

We next discuss the initial conditions. From $\overline{G} = (C^{-1} - \overline{\Sigma})^{-1}$ and $C_{\lambda_\mathrm{i}} = 0$ follows $\overline{G}_{\lambda_\mathrm{i}} = 0$. From Eq. (20), we deduce

$$\overline{\Phi}_{\lambda_\mathrm{i}} = 0, \qquad \overline{\Phi}^{(1)}_{\lambda_\mathrm{i}} = 0, \qquad \overline{\Phi}^{(2)}_{\lambda_\mathrm{i}} = U, \qquad \overline{\Phi}^{(3)}_{\lambda_\mathrm{i}} = 0, \tag{28}$$

$$\begin{aligned} \overline{\Phi}^{(4),\lambda_\mathrm{i}}_{\gamma_1\gamma_2\gamma_3\gamma_4} = -\frac{1}{2} \Big[\Big(\Big\{ \big[U_{\alpha_1\alpha_2\alpha_3\alpha_4} U_{\alpha_1'\alpha_2'\alpha_3'\alpha_4'} + \zeta(\alpha_1 \leftrightarrow \alpha_1') \big] \\ + \zeta(\alpha_2 \leftrightarrow \alpha_2') \Big\} + \zeta(\alpha_3 \leftrightarrow \alpha_3') \Big) + \zeta(\alpha_4 \leftrightarrow \alpha_4') \Big], \end{aligned} \tag{29}$$

and more generally for $n = 1, 2, \ldots$,

$$\overline{\Phi}^{(2n-1)}_{\lambda_\mathrm{i}} = 0, \qquad 0 \neq \overline{\Phi}^{(2n)}_{\lambda_\mathrm{i}} \sim U^n. \tag{30}$$

Note that the nonvanishing result for $\overline{\Phi}^{(4)}_{\lambda_\mathrm{i}}, \overline{\Phi}^{(6)}_{\lambda_\mathrm{i}}, \ldots$ contradicts Ref. [35] where it is claimed that $\overline{\Phi}^{(n)}_{\lambda_\mathrm{i}} = 0$ for $n \geq 3$.

4.2. Truncated flow equations and equivalence to self-consistent perturbation theory

A straightforward truncation of the infinite hierarchy of flow equations for the $\overline{\Phi}^{(n)}$ leading to a closed set of equations is obtained by neglecting the flow of $\overline{\Phi}^{(m)}$ (and higher moments) for some fixed given m by setting $\overline{\Phi}^{(m)}_{\lambda} = \overline{\Phi}^{(m)}_{\lambda_\mathrm{i}}$. As $\overline{\Phi}^{(m)}_{\lambda_\mathrm{i}}$ vanishes for odd m, truncations at level $m = 2l$ and $m = 2l + 1$ are equivalent, yielding both $\overline{\Phi}^{(2l)}_{\lambda} = \overline{\Phi}^{(2l)}_{\lambda_\mathrm{i}} \sim U^l$. As in 1PI fRG, this way of truncating is motivated from a weak coupling perspective: if U is sufficiently small, the impact of the higher moments of $\overline{\Phi}$ on the flow of the lower ones can be neglected. The relation of this truncation to established self-consistent perturbative approximation schemes is discussed next.

The choices $m = 0$ and 1 are pointless since they lead to $\overline{\Phi} = 0, \overline{\Phi}^{(1)} = -\overline{\Sigma} = 0$ during all of the flow. Let us hence consider the case $m = 2$ or 3, which means setting $\overline{\Phi}^{(2)}_{\lambda} = U$. The resulting flow equation $\dot{\overline{\Phi}}^{(1)} = -\dot{\overline{\Sigma}} = U \cdot \dot{\overline{G}}$ can directly be integrated leading to $\overline{\Sigma} = -U \cdot \overline{G}$ which is precisely the Hartree-Fock self-consistency equation for the self-energy. Integration of the flow equation $\dot{\overline{\Phi}} = -\overline{\Sigma} \cdot \dot{\overline{G}} = \overline{G} \cdot U \cdot \dot{\overline{G}}$ in turn yields $\overline{\Phi} = \frac{1}{2} \overline{G} \cdot U \cdot \overline{G}$, which is the first order perturbation theory result for the Luttinger-Ward functional, compare Eq. (20).

Diagrammatic approximations to the Luttinger-Ward functional combined with the self-consistency equation $\Sigma = -\Phi^{(1)}[G]$ are well known [33]. They lead to conserving approximations [33, 32]. In particular, the first order approximation to Φ reproduces self-consistent Hartree-Fock, that is mean-field theory. More generally, the nth order approximation to Φ leads to nth order self-consistent perturbation theory for the self-energy. This means that the self-energy is computed from diagrams up to order U^n, with lines denoting full propagators G that are determined self-consistently.

Now, we observe in general that truncating our set of flow equations at level $m = 2n$ (or, equivalently, $m = 2n+1$) and solving the remaining flow equations results precisely in nth order self-consistent perturbation theory. This holds independently of which λ-dependence is chosen for C, as long as $C_{\lambda_\mathrm{i}} = 0$ and $C_{\lambda_\mathrm{f}} = C$. In particular, this is independent of whether or not C_λ regularizes diagrammatic expressions which are infrared divergent with bare propagators. Furthermore, this is true not only at λ_f but even during all of the flow (if perturbation theory is formulated with C_λ instead of C). For the proof let us denote the nth order perturbation theory approximation to $\Phi[G]$ by $A[G]$. From A being independent of C follows $\dot{A}[G] = 0$ and $\dot{\overline{A}}^{(l)} = \overline{A}^{(l+1)} \cdot \dot{\overline{G}}$. The initial conditions are

$$\overline{A}^{(l)}_{\lambda_\mathrm{i}} = \overline{\Phi}^{(l)}_{\lambda_\mathrm{i}}, l = 0, 1, \ldots, 2n, \qquad \overline{A}^{(l)}_{\lambda_\mathrm{i}} = 0, l \geq 2n+1. \tag{31}$$

Obviously, the hierarchy of flow equations satisfied by the $\overline{A}^{(l)}$ is finite and identical to the truncated exact hierarchy. As $\overline{A}$ and the truncated $\overline{\Phi}$ fulfill the same differential equations and initial conditions, they are the same. This concludes the proof.

We thus derived a fundamental equivalence of two different approaches to the many-body problem: the solution of the 2PI C-flow equations truncated at level $2n$ gives exactly self-consistent perturbation theory to level n. It is rather remarkable that the resummation inherent to the RG procedure leads in the most natural truncation of the 2PI C-flow to a well known conserving approximation. This must be contrasted to most other truncated fRG schemes. E.g. in 1PI fRG, the lowest order truncation for the self-energy is not equivalent to self-consistent Hartree-Fock [1]. Also, the other 2PI fRG schemes discussed here (internally closed C-flow and two U-flow schemes, see below) are not equivalent to self-consistent perturbation theory.

4.3. Internally closed set of flow equations

Given the equivalence of truncated 2PI C-flow and self-consistent perturbation theory, we face the question whether other approximations to the C-flow are conceivable which lead beyond this known approximation to the quantum many-body problem. Such an approximation was studied in Ref. [35], however not motivated by going beyond the above derived equivalence.‖ The idea is to truncate the hierarchy of flow equations for the $\overline{\Phi}^{(n)}$ by finding an approximate expression for $\overline{\Phi}^{(3)}$ in terms of $\overline{\Phi}^{(2)}$. The procedure is based on the leading (second order) perturbative contribution to $\overline{\Phi}^{(3)}$,

$$\left.\overline{\Phi}^{(3)}_{\gamma_1\gamma_2\gamma_3}\right|_{\mathrm{2nd}} = -\frac{1}{2}\sum_{\gamma_4}\Big(\big\{\big[\, U_{\alpha_1\alpha_2\alpha_3\alpha_4}U_{\alpha'_1\alpha'_2\alpha'_3\alpha'_4} + \zeta(\alpha_1 \leftrightarrow \alpha'_1)\big] + \zeta(\alpha_2 \leftrightarrow \alpha'_2)\big\} + \zeta(\alpha_3 \leftrightarrow \alpha'_3)\Big)\,\overline{G}_{\gamma_4}, \tag{32}$$

compare to Eq. (20). In Ref. [35], it is proposed to replace $U \to \overline{\Phi}^{(2)}$ in the expression for $\left.\overline{\Phi}^{(3)}\right|_{\mathrm{2nd}}$. We observe that this idea contains some ambiguity: while U satisfies the full index permutation (anti-)symmetry $U_{\alpha_1\alpha_2\alpha_3\alpha_4} = \zeta^P U_{\alpha_{P1}\alpha_{P2}\alpha_{P3}\alpha_{P4}}$, the symmetry of $\overline{\Phi}^{(2)}$ is only analogous to Eq. (12). In Ref. [35], some specific order of indices of the interaction amplitudes U in Eq. (32) is chosen before replacing $U \to \overline{\Phi}^{(2)}$. Other choices would lead to other approximations. We consider it appropriate to replace instead

---

‖ This equivalence is not observed in Ref. [35], presumably due to the wrong initial conditions [see the sentence following our Eq. (30)].

$$U_{\alpha_1\alpha_2\alpha_3\alpha_4} \to \overline{\Phi}^{(2),\mathrm{sym}}_{\alpha_1\alpha_2\alpha_3\alpha_4} = \frac{1}{3}\left(\overline{\Phi}^{(2)}_{\alpha_1\alpha_2\alpha_3\alpha_4} + \overline{\Phi}^{(2)}_{\alpha_2\alpha_3\alpha_1\alpha_4} + \overline{\Phi}^{(2)}_{\alpha_3\alpha_1\alpha_2\alpha_4}\right), \tag{33}$$

where $\overline{\Phi}^{(2),\mathrm{sym}}$ has the full index permutation (anti-)symmetry. The resulting flow equation,

$$\dot{\overline{\Phi}}^{(2)} = \left(\overline{\Phi}^{(3)}\Big|_{2\mathrm{nd}}\right)_{U\to\overline{\Phi}^{(2),\mathrm{sym}}} \cdot \dot{\overline{G}}, \tag{34}$$

closes the hierarchy. Note that the (anti-)symmetrization of $\overline{\Phi}^{(2)}$ on the right-hand-side of the flow equation is indeed required since $\overline{\Phi}^{(2)}$ resulting from the flow equation does not have the full (anti-)symmetry. We refer to this scheme as "internally closed C-flow".

Due to $\overline{\Phi}^{(2)}_{\lambda_\mathrm{i}} = U$ the flow of $\left(\overline{\Phi}^{(3)}\big|_{2\mathrm{nd}}\right)_{U\to\overline{\Phi}^{(2),\mathrm{sym}}}$ starts at $\overline{\Phi}^{(3)}\big|_{2\mathrm{nd}}$. Integrating the flow equations then leads to

$$\begin{aligned}\overline{\Phi}^{(2)}_{\lambda_\mathrm{f}} &= \overline{\Phi}^{(2)}\Big|_{2\mathrm{nd}} + \mathcal{O}(U^3\overline{G}^4), &(35)\\ \overline{\Sigma}_{\lambda_\mathrm{f}} &= \overline{\Sigma}\big|_{2\mathrm{nd}} + \mathcal{O}(U^3\overline{G}^5), &(36)\\ \overline{\Phi}_{\lambda_\mathrm{f}} &= \overline{\Phi}\big|_{2\mathrm{nd}} + \mathcal{O}(U^3\overline{G}^6), &(37)\end{aligned}$$

where $\overline{\Phi}\big|_{2\mathrm{nd}}$ denotes the contributions to $\overline{\Phi}$ in first and second order in U, compare Eq. (20). Consequently, the solution of the internally closed C-flow comprises second order self-consistent perturbation theory. For the self-energy this means explicitly

$$\overline{\Sigma}_{\lambda_\mathrm{f}} = \overline{\Sigma}_{\mathrm{exact}} + \mathcal{O}(U^3\overline{G}^5_{2\mathrm{SCPT}}), \tag{38}$$

where $\overline{G}_{2\mathrm{SCPT}}$ denotes the full propagator of the physical state in second order self-consistent perturbation theory.

4.4. Computing the thermodynamic potential

One of the key observables depending on the interaction is the expectation value of the energy, which follows from the thermodynamic potential $\Omega[G] = \Gamma[G]/\beta$ with physical value

$$\overline{\Omega} = -\frac{1}{\beta}\ln\overline{Z}. \tag{39}$$

For instance, the ground state energy is $E_{\mathrm{gs}} = \lim_{\beta\to\infty}\overline{\Omega}$.

The thermodynamic potential can be computed from the values of $\overline{\Phi}$ and $\overline{\Sigma}$ that result at the end of the truncated or internally closed C-flow (or which follow in perturbation theory to $\Phi[G]$ from the self-consistency equation $\Phi^{(1)}[\overline{G}] = -\overline{\Sigma} = \overline{G}^{-1} - C^{-1}$). The physical value of the effective action is

$$\overline{\Gamma} = \overline{\Phi} + \Gamma_0[\overline{G}] = \overline{\Phi} - \frac{\zeta}{2}\left[\operatorname{tr}\ln(-\overline{G}) - \operatorname{tr}(C^{-1}\overline{G} - 1)\right]. \tag{40}$$

With $\frac{\zeta}{2}\operatorname{tr}(C^{-1}\overline{G} - 1) = (C^{-1} - \overline{G}^{-1})\cdot\overline{G} = \overline{\Sigma}\cdot\overline{G}$, this means

$$\overline{\Omega} = \frac{1}{\beta}\left[-\frac{\zeta}{2}\operatorname{tr}\ln(-\overline{G}) + \overline{\Phi} + \overline{\Sigma}\cdot\overline{G}\right]. \tag{41}$$

For example in C-flow truncated at level $m = 2$, that is in lowest order perturbation theory to $\Phi[G]$, the resulting self-consistency equation $\overline{\Sigma} = -U \cdot \overline{G}$ corresponds to the mean-field approximation, $\overline{G} = \overline{G}_{\mathrm{MF}}$. From $\Phi_{\mathrm{MF}}[\overline{G}_{\mathrm{MF}}] + \overline{\Sigma}_{\mathrm{MF}} \cdot \overline{G}_{\mathrm{MF}} = -\frac{1}{2}\overline{G}_{\mathrm{MF}} \cdot U \cdot \overline{G}_{\mathrm{MF}}$ follows

$$\overline{\Omega}_{\mathrm{MF}} = \frac{1}{\beta}\left[-\frac{\zeta}{2}\operatorname{tr}\ln(-\overline{G}_{\mathrm{MF}}) - \frac{1}{2}\overline{G}_{\mathrm{MF}} \cdot U \cdot \overline{G}_{\mathrm{MF}}\right] \tag{42}$$

$$= \Omega_0[C]_{C\to\overline{G}_{\mathrm{MF}}} - \frac{1}{2\beta}\overline{G}_{\mathrm{MF}} \cdot U \cdot \overline{G}_{\mathrm{MF}}, \tag{43}$$

which is the well known mean-field result. In order to evaluate $\Omega_0[C]_{C\to\overline{G}_{\mathrm{MF}}}$ one replaces the bare single-particle energies by mean-field dressed energies in the analytic result for $\Omega_0[C] = -(\ln \overline{Z}_0)/\beta$. For the anharmonic oscillator, e.g., one replaces $\omega_{\mathrm{G}} \to \sqrt{\omega_{\mathrm{G}}^2 + \overline{\Sigma}_{\mathrm{MF}}}$ in $\ln \overline{Z}_0 = -\ln[2\sinh(\beta\omega_{\mathrm{G}}/2)]$.

Higher order truncations of the flow produce a frequency dependent $\overline{G}$ which makes the evaluation of $\operatorname{tr}\ln(-\overline{G})$ less trivial. Then, it is convenient to compute the thermodynamic potential from a flow equation instead. Consider any approximation to the flow equations for $\overline{\Phi}^{(1)}, \overline{\Phi}^{(2)}, \ldots$ that result in some function $\overline{\Phi}^{(1)}_{\lambda} = -\overline{\Sigma}_{\lambda}$. This function allows to compute the flow of $\overline{G} = \left(C^{-1} - \overline{\Sigma}\right)^{-1}$ and of $\overline{\Phi}$ as

$$\dot{\overline{G}} = -\overline{G}\left(\dot{C}^{-1} - \dot{\overline{\Sigma}}\right)\overline{G}, \qquad \dot{\overline{\Phi}} = -\overline{\Sigma} \cdot \dot{\overline{G}}. \tag{44}$$

In the same approximation, the flow of $\overline{\Omega}$ is

$$\dot{\overline{\Omega}} = \frac{1}{\beta}\left(\dot{\overline{\Phi}} + \frac{d}{d\lambda}\Gamma_0[\overline{G}]\right) = \frac{1}{\beta}\left(-\overline{\Sigma} \cdot \dot{\overline{G}} + \dot{\Gamma}_0[\overline{G}] + \Gamma_0^{(1)}[\overline{G}] \cdot \dot{\overline{G}}\right). \tag{45}$$

Now $\dot{\Gamma}_0[\overline{G}] = \overline{G} \cdot \dot{C}^{-1}$ and $\Gamma_0^{(1)}[\overline{G}] = C^{-1} - \overline{G}^{-1} = \overline{\Sigma}$ result in

$$\dot{\overline{\Omega}} = \frac{1}{\beta}\overline{G} \cdot \dot{C}^{-1}. \tag{46}$$

We observe that the form of this flow equation is independent of the approximation chosen for the flow of $\overline{\Sigma}_{\lambda}$. Hence, it is valid as well in case of the exact flow, compare Ref. [35].

The initial condition

$$\overline{\Omega}_{\lambda_{\mathrm{i}}} = \frac{1}{\beta}\left(\overline{\Phi} + \Gamma_0[\overline{G}]\right)_{\lambda_{\mathrm{i}}} = -\frac{\zeta}{2\beta}\left[\operatorname{tr}\ln(-\overline{G}) - \operatorname{tr}(C^{-1}\overline{G} - 1)\right]_{\lambda_{\mathrm{i}}} \tag{47}$$

is difficult to handle since $\overline{G}_{\lambda_{\mathrm{i}}} = 0$ leads to a divergence of $\ln(-\overline{G})$. Following Ref. [35], we study instead

$$\Delta\overline{\Omega} = \overline{\Omega} - \Omega_0[C] = \overline{\Omega} + \frac{\zeta}{2\beta}\operatorname{tr}\ln(-C) \tag{48}$$

with initial condition $\Delta\overline{\Omega}_{\lambda_{\mathrm{i}}} = 0$ and flow equation

$$\Delta\dot{\overline{\Omega}} = \frac{d}{d\lambda}\Delta\overline{\Omega} = \dot{\overline{\Omega}} + \frac{\zeta}{2\beta}\frac{d}{d\lambda}\operatorname{tr}\ln(-C) = \frac{1}{\beta}(\overline{G} - C) \cdot \dot{C}^{-1}. \tag{49}$$

At the end of the flow, we recover the thermodynamic potential as $\overline{\Omega}_{\lambda_{\mathrm{f}}} = \Omega_0[C]\big|_{\lambda_{\mathrm{f}}} + \Delta\overline{\Omega}_{\lambda_{\mathrm{f}}}$.

4.5. Application to the anharmonic oscillator

We test the performance of C-flow truncated at level $m = 2, 4$ or internally closed on the quantum anharmonic oscillator (with $\zeta = +$ and $\alpha = \tau$). Due to translational invariance in imaginary time, it is preferable to work in frequency representation. Hence, we Fourier transform the m-point functions to bosonic Matsubara frequencies $\omega_n = \frac{2\pi}{\beta} n$,

$$W^{(m)}_{n_1 n_1' \dots n_m n_m'} = \int_{\tau_1} \dots \int_{\tau_m'} e^{-i\omega_{n_1}\tau_1 \dots - i\omega_{n_m}\tau_m} W^{(m)}\left(\tau_1, \dots, \tau_m'\right) e^{-i\omega_{n_1'}\tau_1' \dots - i\omega_{n_m'}\tau_m'}, \quad (50)$$

$$\Phi^{(m)}_{n_1 n_1' \dots n_m n_m'} = \int_{\tau_1} \dots \int_{\tau_m'} e^{+i\omega_{n_1}\tau_1 \dots + i\omega_{n_m}\tau_m} \Phi^{(m)}\left(\tau_1, \dots, \tau_m'\right) e^{+i\omega_{n_1'}\tau_1' \dots + i\omega_{n_m'}\tau_m'}, \quad (51)$$

where $\int_\tau = \int_0^\beta d\tau$. Mind the choice of signs in the exponents. Here, $W^{(m)}$ is a representative of propagators (including G), whereas $\Phi^{(m)}$ represents vertices (including Σ). For the free inverse propagator one obtains

$$\left(C^{-1}\right)_{nn'} = -\beta\delta_{n+n',0}\left(i\omega_n i\omega_{n'} + \omega_{\mathrm{G}}^2\right) = -\beta\delta_{n+n',0}\left(\omega_n^2 + \omega_{\mathrm{G}}^2\right). \quad (52)$$

More generally, all relevant functions are proportional to $\beta\delta_{n_1+\dots,0}$. We refer to the remaining part by skipping the last index, e.g.

$$\Sigma_{nn'} = \beta\delta_{n+n',0}\Sigma_n, \qquad \Phi^{(2)}_{n_1 n_1' n_2 n_2'} = \beta\delta_{n_1+n_1'+n_2+n_2',0}\Phi^{(2)}_{n_1 n_1' n_2}. \quad (53)$$

For the flow parameter dependence of C, we choose specifically

$$C_n^\lambda = -\left(\omega_n^2 + \omega_{\mathrm{G}}^2 + \lambda\right)^{-1}, \quad (54)$$

with $\lambda_{\mathrm{i}} = \infty$ and $\lambda_{\mathrm{f}} = 0$. This can be considered as an analogue to the so-called hybridization flow parameter for single-level quantum impurity problems [49, 14, 15], which has the form $C_n^\lambda = \left[i\omega_n - \varepsilon + i\,\mathrm{sgn}(\omega_n)(\Gamma + \lambda)\right]^{-1}$ for a system in grand canonical equilibrium. Here, ε denotes the on-site energy of the level and Γ the hybridization to the leads. Generally speaking, the results following from the solution of truncated fRG flow equations depend on the cutoff choice (in contrast to the solution of the infinite hierarchy of equations) [1]. Therefore, it is an interesting observation that the results of truncated C-flow are completely independent of the particular choice of the flow parameter as they are equivalent to self-consistent perturbation theory. This does not hold for the internally closed C-flow. By comparison to exact results, it was shown for selected fermionic many-body models that the hybridization flow parameter is a good choice [14, 15] in 1PI fRG. This provides the motivation to use its analogue for the problem at hand. We here do not further investigate the influence of the cutoff choice on the quality of the results.

Dyson's equation yields

$$\overline{G}_n = \left[(C^{-1})_n - \overline{\Sigma}_n\right]^{-1} = -\left(\omega_n^2 + \omega_{\mathrm{G}}^2 + \lambda + \overline{\Sigma}_n\right)^{-1}. \quad (55)$$

Due to $\dot{C}_n^{-1} = -1$ the flow equation (49) for the thermodynamic potential takes the form

$$\Delta\dot{\overline{\Omega}} = -\frac{1}{2\beta}\sum_n \left(\overline{G}_n - C_n\right). \quad (56)$$

The flow of the self-energy $\overline{\Sigma} = -\overline{\Phi}^{(1)}$ reads

$$\dot{\overline{\Sigma}}_{n_1} = -\frac{1}{2\beta}\sum_{n_3} \overline{\Phi}^{(2)}_{n_1,-n_1,n_3}\dot{\overline{G}}_{n_3}, \quad (57)$$

with

$$\dot{\overline{G}}_n = -\overline{G}_n \left[(\dot{C}^{-1})_{-n} - \dot{\overline{\Sigma}}_{-n} \right] \overline{G}_n. \tag{58}$$

The initial conditions are $\overline{\Sigma}_n^{\lambda_\mathrm{i}} = 0$ and $\overline{\Phi}^{(2),\lambda_\mathrm{i}}_{n_1 n_1' n_2} = g$. In case of C-flow truncated at level $m = 4$, the solution is self-consistent second order perturbation theory,

$$\overline{\Sigma}_{n_1} = -\frac{g}{2\beta} \sum_{n_2} \overline{G}_{n_2} + \frac{g^2}{6\beta^2} \sum_{n_2 n_3} \overline{G}_{n_2} \overline{G}_{n_3} \overline{G}_{-n_1-n_2-n_3}. \tag{59}$$

This equation is solved self-consistently for each λ (which is numerically faster and more accurate than integrating the flow of $\overline{\Sigma}$, $\overline{\Phi}^{(2)}$ and $\overline{\Phi}^{(3)}$) and the result is used to calculate the flow of $\Delta\overline{\Omega}$.

For the internally closed C-flow, Eq. (57) is solved numerically together with

$$\dot{\overline{\Phi}}^{(2)}_{n_1 n_1' n_2} = -\frac{1}{\beta} \sum_{n_3} \left\{ \overline{\Phi}^{(2),\mathrm{sym}}_{n_1,n_2,n_3} \overline{\Phi}^{(2),\mathrm{sym}}_{n_1',n_2',n_3'} \overline{G}_{n_1+n_2+n_3} + (n_1 \leftrightarrow n_1') \right\} \Big|^{n_2' = -n_1 - n_1' - n_2}_{n_3' = -n_3} \dot{\overline{G}}_{n_3}, \tag{60}$$

$$\overline{\Phi}^{(2),\mathrm{sym}}_{n_1,n_2,n_3} = \frac{1}{3} \left(\overline{\Phi}^{(2)}_{n_1,n_2,n_3} + \overline{\Phi}^{(2)}_{n_2,n_3,n_1} + \overline{\Phi}^{(2)}_{n_3,n_1,n_2} \right). \tag{61}$$

Eq. (60) exploits the symmetry $\overline{\Sigma}_{n_1} = \overline{\Sigma}_{-n_1}$ which implies $\overline{G}_{n_1} = \overline{G}_{-n_1}$. It follows from Eq. (12), which translates to $\overline{\Phi}^{(2)}_{n_1 n_1' n_2} = \overline{\Phi}^{(2)}_{n_1' n_1 n_2}$ in frequency space, via Eq. (57).

We restrict our numerical investigations to the case of vanishing temperature and thus take the limit $\beta \to \infty$. The Matsubara frequencies become continuous then, $\omega_n \to \nu$, and sums turn into integrals, $\frac{1}{\beta}\sum_n \to \int \frac{d\nu}{2\pi}$. Transforming, for instance, Eq. (59), one finds explicitly

$$\overline{\Sigma}(\nu) = -\frac{g}{2} \int_{-\infty}^{\infty} \frac{d\nu_1}{2\pi} \overline{G}(\nu_1) + \frac{g^2}{6} \int_{-\infty}^{\infty} \frac{d\nu_2}{2\pi} \int_{-\infty}^{\infty} \frac{d\nu_3}{2\pi} \overline{G}(\nu_2) \overline{G}(\nu_3) \overline{G}(-\nu - \nu_2 - \nu_3). \tag{62}$$

We here focus on two observables. One is the shift in the ground state energy induced by the anharmonicity, $e_\mathrm{gs} = E_\mathrm{gs} - E^0_\mathrm{gs} = \lim_{\beta\to\infty} \Delta\overline{\Omega}$, with the non-interacting ($g = 0$) ground state energy E^0_gs. The other is the fluctuation of the position $\varrho = \langle x^2 \rangle$ which corresponds to the particle density in a fermionic many-body problem. In the following we therefore refer to ϱ as the density. At the end of the flow, it can be extracted from the self-energy as

$$\varrho = -\overline{G}(0,0) = \int_{-\infty}^{\infty} \frac{d\nu}{2\pi} \frac{1}{\nu^2 + \omega_\mathrm{G}^2 + \overline{\Sigma}(\nu)} \approx \int_0^{\nu_{m_\mathrm{len}}} \frac{d\nu}{\pi} \frac{1}{\nu^2 + \omega_\mathrm{G}^2 + \overline{\Sigma}(\nu)} + \frac{1}{\pi \nu_{m_\mathrm{len}}}. \tag{63}$$

Here, the last integral refers to the numerical evaluation on a grid of frequencies ν_n with $n = -m_\mathrm{len}, \ldots, m_\mathrm{len}$ and $\nu_n = -\nu_{-n}$ (details on the grid are given in Appendix A). The integral is then calculated by an interpolator. The very last addend is an approximation to the missing integral part $-\int_{\nu_{m_\mathrm{len}}}^{\infty} \frac{d\nu}{\pi} \overline{G}(\nu)$.

In case of C-flow truncated at level $m = 2$, the solution is mean-field theory. At zero temperature, the self-consistency equation $\overline{\Sigma}_\mathrm{MF} = -U \cdot \overline{G}_\mathrm{MF}$ takes the form

$$\overline{\Sigma}_\mathrm{MF} = \frac{g}{2} \langle x^2 \rangle_\mathrm{MF} = \frac{g}{4} \frac{1}{\sqrt{\omega_\mathrm{G}^2 + \overline{\Sigma}_\mathrm{MF}}}. \tag{64}$$

In this case, we do not integrate numerically any flow but solve the self-consistency equation directly at λ_f and compute the thermodynamic potential from Eq. (43) (taking $\beta \to \infty$). This leads to the regular mean-field result [4]

$$e^\mathrm{MF}_\mathrm{gs} = \frac{1}{2} \sqrt{\omega_\mathrm{G}^2 + \overline{\Sigma}_\mathrm{MF}} - \frac{1}{2g} \overline{\Sigma}^2_\mathrm{MF} - \frac{\omega_\mathrm{G}}{2}. \tag{65}$$

For the internally closed C-flow, $\overline{\Phi}_{\lambda}^{(2)}$ depends on three frequencies. Consequently, the number of flow equations scales $\sim m_{\mathrm{len}}^{3}$. As one sum must be performed on the right-hand-side of Eq. (60), the effort of computing all the right-hand-sides of the set of differential equations in each step of the flow scales $\sim m_{\mathrm{len}}^{4}$. This severely limits the accessible m_{len} in this scheme. In comparison, the regular C-flow schemes truncated at arbitrary order m always produce $\sim m_{\mathrm{len}}$ number of flow equations. This is because only $\Delta\overline{\Omega}$ and $\overline{\Sigma}(\nu)$ flow in the regular schemes as the flow of $\overline{\Sigma}(\nu)$ can be determined self-consistently. Nevertheless, there is (of course) an increasing cost for calculating increasing orders m: the effort to calculate the right-hand-side of the self-consistency equation for $\overline{\Sigma}(\nu)$ increases. For example at $m = 4$, the effort to calculate all equations for one step of the flow is $\sim m_{\mathrm{len}}^{2}$—this can be managed by pre-calculating one of the $d\nu_2, d\nu_3$-integrals in Eq. (62) before actually calculating the right-hand-side of the equation itself.

4.6. Numerical results for the anharmonic oscillator

For all numerical considerations, ω_{G} is set to 1 in this paper. Fig. 2 shows numerical results for the ground state energy shift and the density as functions of the coupling constant g. The data obtained from C-flow truncated at levels $m = 2, 4$ or internally closed are compared to the exact results. As the actual ("absolute") curves are very close to each other, the main plots show the relative differences to the exact result.

We compute the numerically exact data by matrix diagonalization: the full Hamiltonian (with quartic anharmonicity) can be expressed as a matrix in the basis of the energy eigenstates $\left|E_n^0\right\rangle$ of the unperturbed harmonic oscillator. Diagonalizing this matrix yields the energy eigenvalues and eigenstates of the anharmonic system. The ground state density is then obtained as $\varrho_{\mathrm{gs}}^{\mathrm{exact}} = \langle E_0|\, \hat{x}^2 \,|E_0\rangle$, where the matrix $(\hat{x}^2)_{m,n} = \left\langle E_m^0\right|\hat{x}^2\left|E_n^0\right\rangle$ in the unperturbed eigenbasis only has the following non-zero elements: $(\hat{x}^2)_{n,n} = n + \frac{1}{2}$ and $(\hat{x}^2)_{n+2,n} = (\hat{x}^2)_{n,n+2} = \frac{1}{2}\sqrt{n+1}\sqrt{n+2}$. This can easily be proven from the ladder operator representation $\hat{x} = \left(\hat{a} + \hat{a}^{\dagger}\right)/\sqrt{2}$. A matrix size of 200×200 is found to be sufficient for converged numerics.

In all numerical C-flow computations, the frequency grid covers the range from $\nu_{-m_{\mathrm{len}}} = -5120$ to $\nu_{m_{\mathrm{len}}} = 5120$ with $2m_{\mathrm{len}} + 1$ grid points, see Appendix A for details on the grid. The truncated C-flow is computed with $m_{\mathrm{len}} = 500$, while the numerically much more demanding internally closed C-flow is solved with $m_{\mathrm{len}} = 45$. In the latter case, comparison to $m_{\mathrm{len}} = 35$ and 40 data suggests that convergence was reached on the scale of the figure.¶ This is also supported by the observation that data from truncated C-flow computed at $m_{\mathrm{len}} = 45$ are close to their converged counter-parts. For all C-flow methods, the flow starts at $\lambda_{\mathrm{i}}^{\mathrm{num}} = 10^{16}$. Convergence with respect to $\lambda_{\mathrm{i}}^{\mathrm{num}}$ requires such a large value since the ground state energy depends on $\lambda_{\mathrm{i}}^{\mathrm{num}}$ in leading order via an addend proportional to $1/\sqrt{\lambda_{\mathrm{i}}^{\mathrm{num}}}$.

Obviously, the self-consistent Hartree-Fock approximation, that is C-flow truncated at $m = 2$, yields already quite good results with a relative discrepancy of less than 3% for g up to 50. For the problem at hand, this is plausible as mean-field theory can be expected to capture reasonably well the effect of the x^4-anharmonicity on low-energy properties by self-consistently optimizing the frequency of the harmonic oscillator. The improvement achieved by second order self-consistent perturbation theory, that is C-flow truncated at $m = 4$, is rather low in comparison: the data is

---

¶ If at all, the energy curve is expected to move a little closer towards the exact data for higher m_{len}.

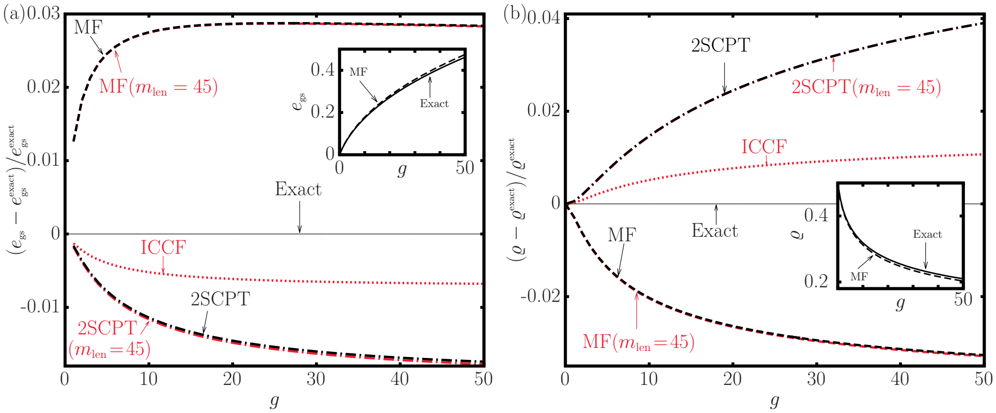

Figure 2. Numerical results for the ground state energy e_{gs} (a) and the density ϱ (b) as a function of the strength of the anharmonicity g. The lines show data obtained from C-flow truncated at level $m = 2$ (dashed), that is mean-field theory (MF), from C-flow truncated at level $m = 4$ (dashed-dotted), that is second order self-consistent perturbation theory (2SCPT), and from internally closed C-flow (dotted; ICCF). The main plots show the relative difference to the exact result, whereas the insets show the absolute mean-field and exact curves.

typically 1 to 2% off for e_{gs}, while ϱ is reproduced even less accurate than by the Hartree-Fock approximation for $g \gtrsim 20$. The results from internally closed C-flow are significantly better, with relative deviations below 1% for both observables. The idea of internally closing the set of differential equations by expressing $\overline{\Phi}^{(3)}$ in terms of $\overline{\Phi}^{(2)}$ is thus the most successful C-flow scheme investigated here. However, the price to pay is a large computational effort $\sim m_{\text{len}}^4$ for the computation of the set of differential equations in each step of the flow. Additionally, it is unclear whether this approach can be systematically generalized to higher orders. Therefore, it is not possible to compare results from truncations at different orders in order to assess the quality of a given approximation, a procedure often used in fRG studies [1]. Anyhow, hypothetical higher orders of internally closed C-flow seem out of reach for numerical computations as the scheme implemented here is already numerically quite demanding.

The question emerges whether one can think of an RG scheme that better fits the 2PI nature of the general approach. One possible answer is the U-flow that shall be discussed in Sect. 6. Sect. 5 provides some preliminaries for this discussion.

5. Pair propagator and Bethe-Salpeter equation

In the discussion of the U-flow scheme below, some notions related to four-point functions and the dot-product introduced above will be useful. They are provided in this section which can be considered as a sequel to Sect. 3.

From the non-interacting functional $W_0[J] = -\frac{\zeta}{2}\,\mathrm{tr}\ln(-C^{-1} - J)$ follows $G_0[J] = -W_0^{(1)}[J] = (C^{-1} + J)^{-1}$. From $W_0^{(2)}[J] = -\delta G_0[J]/\delta J$ follows $W_0^{(2)}\big[J_0[G]\big] = \Pi[G]$, with the pair propagator

$$\Pi_{\gamma_1\gamma_2}[G] = -\frac{\delta G_{\gamma_2}}{\delta G^{-1}_{\gamma_1}} = G_{\alpha_2\alpha_3}\frac{\delta G^{-1}_{\alpha_3\alpha'_3}}{\delta G^{-1}_{\alpha_1\alpha'_1}}G_{\alpha'_3\alpha'_2} = G_{\alpha'_1\alpha_2}G_{\alpha_1\alpha'_2} + \zeta G_{\alpha_1\alpha_2}G_{\alpha'_1\alpha'_2}. \tag{66}$$

In case of a particle number conserving system, Π denotes either a particle-hole or a particle-particle propagator, depending on the charge indices. For example the charge indices $c_1 = -c_1' = c_2 = -c_2'$ render $\Pi_{\gamma_1\gamma_2}$ a particle-hole propagator, while the charge indices $c_1 = c_1' = -c_2 = -c_2'$ lead to a particle-particle propagator.

In the general interacting case, one has

$$W^{(2)} \cdot \Gamma^{(2)} = \frac{\delta W^{(1)}}{\delta J} \cdot \frac{\delta \Gamma^{(1)}}{\delta G} = \frac{\delta G}{\delta J} \cdot \frac{\delta J}{\delta G} = \frac{\delta J}{\delta J} = I, \tag{67}$$

where

$$I_{\gamma_1\gamma_2} = \frac{\delta J_{\gamma_2}}{\delta J_{\gamma_1}} = \delta_{\alpha_1\alpha_2}\delta_{\alpha_1'\alpha_2'} + \zeta \delta_{\alpha_1\alpha_2'}\delta_{\alpha_1'\alpha_2} \tag{68}$$

is the neutral element with respect to the dot-product, $X \cdot I = I \cdot X = X$. We conclude

$$W^{(2)} = \left(\Gamma^{(2)}\right)^{\mathrm{inv}}, \tag{69}$$

and in particular $\Gamma_0^{(2)} = \Pi^{\mathrm{inv}}$. Here, we introduced the dot-product inverse of four-point functions that satisfies

$$\left(X \cdot X^{\mathrm{inv}}\right)_{\gamma_1\gamma_2} = \frac{1}{2}\sum_{\gamma_3} X_{\gamma_1\gamma_3} X^{\mathrm{inv}}_{\gamma_3\gamma_2} = I_{\gamma_1\gamma_2}. \tag{70}$$

An example is

$$\left(\Pi^{\mathrm{inv}}\right)_{\gamma_1\gamma_2}[G] = G^{-1}_{\alpha_1'\alpha_2} G^{-1}_{\alpha_1\alpha_2'} + \zeta G^{-1}_{\alpha_1\alpha_2} G^{-1}_{\alpha_1'\alpha_2'}, \tag{71}$$

where G^{-1} denotes the regular inverse with respect to the α-indices. Now, $\Gamma^{(2)} = \Phi^{(2)} + \Gamma_0^{(2)} = \Phi^{(2)} + \Pi^{\mathrm{inv}}$ leads to the Bethe-Salpeter equation

$$W^{(2)} = \left(\Pi^{\mathrm{inv}} + \Phi^{(2)}\right)^{\mathrm{inv}} = \Pi - \Pi \cdot \Phi^{(2)} \cdot \Pi \pm \ldots = \Pi - \Pi \cdot \Phi^{(2)} \cdot W^{(2)}. \tag{72}$$

6. U-flow

6.1. Flow parameter, flow equations, and initial conditions for the plain U-flow

In 1PI fRG, the flow parameter is typically introduced in the one-particle propagator. In C-flow, this procedure was carried over to the 2PI case. We next explore the consequences of introducing the flow parameter into the interaction, $U \to U_\lambda$, as done in Ref. [36]. This method will be denoted as "U-flow". We set $U_{\lambda_{\mathrm{i}}} = 0$ at the beginning of the flow, such that the flow starts at the non-interacting model. At the end of the flow, $U_{\lambda_{\mathrm{f}}} = U$ restores the original interacting problem. We maintain the full index permutation (anti-)symmetry of the interaction during all of the flow, such that $\dot{U}_{\alpha_1\alpha_2\alpha_3\alpha_4} = \zeta^P \dot{U}_{\alpha_{P1}\alpha_{P2}\alpha_{P3}\alpha_{P4}}$.

In Ref. [7], an "interaction flow" method in the framework of 1PI fRG was studied. The authors describe that a flow parameter $C \to \lambda C$ can be substituted to a flow parameter $U \to \lambda^2 U$ by rescaling the fields. One could jump to the conclusion that there is in principle no difference between C-flow and U-flow, at least for a multiplicative flow parameter. The rescaling of the fields, however, leads to a λ-dependent rescaling of all Green and vertex functions. Thus, the structure of the flow equations for the non-rescaled vertex functions differs for the two flow parameters and suggests different truncation procedures.

It is conceivable to combine the C-flow and U-flow schemes by introducing a flow parameter into both, C and U, compare Ref. [36] and also [46]. Here, we discuss only the pure U-flow. In a combined scheme, the flow equations will include additionally the terms derived for the C-flow in Sect. 4.1.

Possible infrared divergencies of perturbation theory ought to be regularized by the chosen flow parameter. This can indeed be achieved in the framework of the U-flow. It has been shown e.g. in the context of partial bosonization for one-dimensional models with interactions that involve only small momentum transfers that a cutoff in this transfer regularizes all infrared divergencies [50] (see also [36]).

U_λ induces a λ-dependence of the action and of the functionals. We now derive the flow equations for the $\overline{\Phi}_\lambda^{(n)}$. We refer to this scheme as "plain U-flow" in order to distinguish it from the modified scheme that is proposed in Ref. [36] and which we describe in Sect. 6.3. The flow of the functionals is given by

$$\dot{Z} = -\frac{1}{3!}\,\mathrm{Tr}\,\dot{U}\cdot\frac{\delta^2 Z}{\delta J\delta J}, \tag{73}$$

$$\dot{W} = \frac{\dot{Z}}{Z} = -\frac{1}{3!}\left[\mathrm{Tr}\left(\dot{U}\cdot W^{(2)}\right) + W^{(1)}\cdot\dot{U}\cdot W^{(1)}\right], \tag{74}$$

$$\dot{\Gamma} = -\dot{W}|_{J[G]} = \frac{1}{3!}\left[\mathrm{Tr}\left(\dot{U}\cdot W^{(2)}\right) + G\cdot\dot{U}\cdot G\right]. \tag{75}$$

In the last expression, $W^{(2)}\big[J[G]\big] = \big(\Gamma^{(2)}[G]\big)^{\mathrm{inv}}$. We used the "double-index" trace

$$\mathrm{Tr}\,X = \frac{1}{2}\sum_\gamma X_{\gamma\gamma}, \tag{76}$$

compare Ref. [36], which is to be distinguished from the "single-index" trace $\mathrm{tr}\,Y = \sum_\alpha Y_{\alpha\alpha}$. As the non-interacting effective action Γ_0 does not depend on U, the flow of the Luttinger-Ward functional $\Phi = \Gamma - \Gamma_0$ is given by

$$\dot{\Phi} = \dot{\Gamma} = \frac{1}{3!}\,\mathrm{Tr}\,\dot{U}\cdot\left(W^{(2)} + \frac{\Pi}{2}\right), \tag{77}$$

where $W^{(2)} = \big(\Pi^{\mathrm{inv}} + \Phi^{(2)}\big)^{\mathrm{inv}}$.

In order to compute the flow of the $\overline{\Phi}^{(n)}$ given by $\dot{\overline{\Phi}}^{(n)} = \overline{\dot{\Phi}}^{(n)} + \overline{\Phi}^{(n+1)}\cdot\dot{\overline{G}}$, we need expressions for $\dot{\overline{G}}$ and $\dot{\Phi}^{(n)}$. For $\dot{\overline{G}}$, we use Eq. (26) for the practical application to the anharmonic oscillator. However, for gaining general analytical insights, a different but equivalent expression turns out to be useful: from $0 = \dot{\overline{\Gamma}}^{(1)} = \overline{\dot{\Gamma}}^{(1)} + \overline{\Gamma}^{(2)}\cdot\dot{\overline{G}}$ follows

$$\dot{\overline{G}} = -\big(\overline{\Gamma}^{(2)}\big)^{\mathrm{inv}}\cdot\overline{\dot{\Gamma}}^{(1)} = -\overline{W}^{(2)}\cdot\overline{\dot{\Phi}}^{(1)}. \tag{78}$$

For $\dot{\Phi}^{(1)} = \delta\dot{\Phi}/\delta G$, we find

$$\begin{aligned}\dot{\Phi}^{(1)} &= \frac{1}{3!}\,\mathrm{Tr}\,\dot{U}\cdot\left(\frac{\delta W^{(2)}}{\delta G} + \frac{1}{2}\frac{\delta\Pi}{\delta G}\right) &(79)\\ &= \frac{1}{3!}\,\mathrm{Tr}\,\dot{U}\cdot\left[W^{(2)}\cdot\left(\Pi^{\mathrm{inv}}\cdot\frac{\delta\Pi}{\delta G}\cdot\Pi^{\mathrm{inv}} - \Phi^{(3)}\right)\cdot W^{(2)} + \frac{1}{2}\frac{\delta\Pi}{\delta G}\right]; &(80)\end{aligned}$$

writing indices explicitly, this means

$$\begin{aligned}\dot{\Phi}^{(1)}_{\gamma_1} = \frac{1}{3}\sum_{\gamma_2}&\left(\Pi^{\mathrm{inv}}\cdot W^{(2)}\cdot\dot{U}\cdot W^{(2)}\cdot\Pi^{\mathrm{inv}} + \frac{\dot{U}}{2}\right)_{\alpha_1\alpha_2\alpha_2'\alpha_1'} G_{\gamma_2}\\ &- \frac{1}{4!}\sum_{\gamma_2\gamma_3}\Phi^{(3)}_{\gamma_1\gamma_2\gamma_3}\left(W^{(2)}\cdot\dot{U}\cdot W^{(2)}\right)_{\gamma_3\gamma_2}. \end{aligned}\tag{81}$$

This yields explicit expressions for $\dot{\overline{G}} = -\overline{W}^{(2)} \cdot \overline{\dot{\Phi}}^{(1)}$, and

$$\dot{\overline{\Phi}} = \overline{\dot{\Phi}} + \overline{\Phi}^{(1)} \cdot \dot{\overline{G}} = \overline{\dot{\Phi}} - \overline{\Phi}^{(1)} \cdot \overline{W}^{(2)} \cdot \overline{\dot{\Phi}}^{(1)}, \tag{82}$$

as well as

$$\dot{\overline{\Phi}}^{(1)} = \overline{\dot{\Phi}}^{(1)} + \overline{\Phi}^{(2)} \cdot \dot{\overline{G}} = \left(I - \overline{\Phi}^{(2)} \cdot \overline{W}^{(2)}\right) \cdot \overline{\dot{\Phi}}^{(1)} = \left(I + \overline{\Phi}^{(2)} \cdot \overline{\Pi}\right)^{\mathrm{inv}} \cdot \overline{\dot{\Phi}}^{(1)}. \tag{83}$$

In order to evaluate the right-hand-side of Eqs. (82) and (83), we need to know $\overline{\Phi}^{(1)}$, $\overline{\Phi}^{(2)}$ [which also allows to compute $\overline{W}^{(2)} = \left(\overline{\Pi}^{\mathrm{inv}} + \overline{\Phi}^{(2)}\right)^{\mathrm{inv}}$], and $\overline{\Phi}^{(3)}$ [cf. Eq. (81)]. This is the onset of an infinite hierarchy of coupled flow equations, where $\dot{\overline{\Phi}}$ depends on $\overline{\Phi}^{(1)}, \dots, \overline{\Phi}^{(3)}$, and where $\dot{\overline{\Phi}}^{(n)}$ depends on $\overline{\Phi}^{(2)}, \dots, \overline{\Phi}^{(n+2)}$ for $n \geq 1$.

The starting point of the flow is given by $U_{\lambda_{\mathrm{i}}} = 0$ and corresponds to the non-interacting model. Consequently, $\Phi_{\lambda_{\mathrm{i}}} = 0$ and

$$\overline{\Phi}_{\lambda_{\mathrm{i}}} = 0, \qquad \overline{\Phi}^{(n)}_{\lambda_{\mathrm{i}}} = 0,\ n = 1, 2, 3, \dots \tag{84}$$

The flow of the thermodynamic potential is given by

$$\dot{\overline{\Omega}} = \frac{\dot{\overline{\Gamma}}}{\beta} = \frac{1}{\beta}\left(\overline{\dot{\Gamma}} + \overline{\Gamma}^{(1)} \cdot \dot{\overline{G}}\right) = \frac{\overline{\dot{\Gamma}}}{\beta} = \frac{\overline{\dot{\Phi}}}{\beta}. \tag{85}$$

It starts at the non-interacting potential, $\overline{\Omega}_{\lambda_{\mathrm{i}}} = \Omega_0[C] = -\frac{1}{\beta} \ln \overline{Z}_0$.

6.2. Truncation of the plain U-flow

In the plain U-flow, the lowest truncation of the hierarchy of flow equations that leads to a flowing self-energy is at level $m = 3$: one sets $\overline{\Phi}^{(n)}_{\lambda} = \overline{\Phi}^{(n)}_{\lambda_{\mathrm{i}}} = 0$, that is to its initial value, for $n \geq 3$. The resulting flow equation $\dot{\overline{\Phi}}^{(2)} = \overline{\dot{\Phi}}^{(2)} + \overline{\Phi}^{(3)} \cdot \dot{\overline{G}} = \overline{\dot{\Phi}}^{(2)}$ reads

$$\begin{aligned}\dot{\overline{\Phi}}^{(2)} = \frac{1}{3!} \operatorname{Tr} \dot{U} \Bigg[& 2\overline{W}^{(2)} \cdot \overline{\Pi}^{\mathrm{inv}} \cdot \frac{\delta \overline{\Pi}}{\delta \overline{G}} \cdot \left(\overline{\Pi}^{\mathrm{inv}} \cdot \overline{W}^{(2)} \cdot \overline{\Pi}^{\mathrm{inv}} - \overline{\Pi}^{\mathrm{inv}}\right) \cdot \frac{\delta \overline{\Pi}}{\delta \overline{G}} \cdot \overline{\Pi}^{\mathrm{inv}} \cdot \overline{W}^{(2)} \\ & + \overline{W}^{(2)} \cdot \overline{\Pi}^{\mathrm{inv}} \cdot \frac{\delta^2 \overline{\Pi}}{\delta \overline{G}^2} \cdot \overline{\Pi}^{\mathrm{inv}} \cdot \overline{W}^{(2)} + \frac{1}{2} \frac{\delta^2 \overline{\Pi}}{\delta \overline{G}^2} \Bigg]\end{aligned} \tag{86}$$

and produces a $\overline{\Phi}^{(2)}$ with explicit time or frequency dependence that enters the flow of the self-energy. Solving the flow equations is then already quite involved. In order to find a simpler approximation, we use the expansion $\overline{W}^{(2)} = \overline{\Pi} + \mathcal{O}\left(\overline{\Phi}^{(2)}\right)$ and get

$$\dot{\overline{\Phi}}^{(2)} = \frac{1}{4} \operatorname{Tr} \dot{U} \cdot \frac{\delta^2 \overline{\Pi}}{\delta \overline{G}^2} + \mathcal{O}\left(\dot{U} \overline{\Phi}^{(2)}\right) = \dot{U}\left[1 + \mathcal{O}\left(\overline{\Phi}^{(2)}\right)\right]. \tag{87}$$

This can be integrated to $\overline{\Phi}^{(2)}_{\lambda} = U_{\lambda} + \mathcal{O}(U_{\lambda}^2)$ which we approximate by $\overline{\Phi}^{(2)}_{\lambda} = U_{\lambda}$. This result can be understood also as the leading perturbative approximation to $\Phi^{(2)}$, compare Eq. (20). The flow equations for the self-energy and the thermodynamic potential are then

$$\begin{aligned}\dot{\overline{\Sigma}}^{\lambda}_{\gamma_1} = -\frac{1}{6} \sum_{\gamma_2, \gamma_3} & (I + U_{\lambda} \cdot \overline{\Pi}_{\lambda})^{\mathrm{inv}}_{\gamma_1 \gamma_2} \\ & \times \left[(I + U_{\lambda} \cdot \overline{\Pi}_{\lambda})^{\mathrm{inv}} \cdot \dot{U}_{\lambda} \cdot (I + \overline{\Pi}_{\lambda} \cdot U_{\lambda})^{\mathrm{inv}} + \frac{\dot{U}_{\lambda}}{2}\right]_{\alpha_2 \alpha_3 \alpha_3' \alpha_2'} \overline{G}^{\lambda}_{\gamma_3},\end{aligned} \tag{88}$$

$$\dot{\overline{\Omega}}_\lambda = \frac{1}{3!\beta}\,\mathrm{Tr}\,\dot{U}_\lambda \cdot \left[\left(\overline{\Pi}_\lambda^{\mathrm{inv}} + U_\lambda\right)^{\mathrm{inv}} + \frac{\overline{\Pi}_\lambda}{2}\right]. \tag{89}$$

Let us address the question how the solutions of these approximate flow equations compare to perturbation theory. It turns out that they comprise first and second order perturbation theory (with bare propagators),

$$\overline{\Sigma}_{\lambda_\mathrm{f}} = \overline{\Sigma}_{\mathrm{exact}} + \mathcal{O}\left(U^3\right), \qquad \overline{\Omega}_{\lambda_\mathrm{f}} = \overline{\Omega}_{\mathrm{exact}} + \mathcal{O}\left(U^3\right). \tag{90}$$

For the proof, we start from the initial condition $\overline{\Sigma}_{\lambda_\mathrm{i}} = 0$, $\overline{G}_{\lambda_\mathrm{i}} = C$, $\overline{\Pi}_{\lambda_\mathrm{i}} = \overline{\Pi}_0$. From $\dot{\overline{\Sigma}} = \mathcal{O}(\dot{U})[1 + \mathcal{O}(U)]$ follows $\overline{\Sigma} = \mathcal{O}(U)$, hence $\overline{G} = C + \mathcal{O}(U)$, $\overline{\Pi} = \overline{\Pi}_0 + \mathcal{O}(U)$. This leads to

$$\begin{aligned}\dot{\overline{\Sigma}}_{\gamma_1} = \big[&-\dot{U}\cdot C - \dot{U}\cdot(C\overline{\Sigma}C) + U\cdot\overline{\Pi}_0\cdot\dot{U}\cdot C\big]_{\gamma_1} \\ &+ \frac{1}{3}\sum_{\gamma_3}(U\cdot\overline{\Pi}_0\cdot\dot{U} + \dot{U}\cdot\overline{\Pi}_0\cdot U)_{\alpha_1\alpha_3\alpha'_3\alpha'_1}C_{\gamma_3} + \mathcal{O}(U^2\dot{U}).\end{aligned} \tag{91}$$

The first addend can be integrated to $(-U\cdot C)$ which is first order perturbation theory for $\overline{\Sigma}$. We insert $\overline{\Sigma} = -U\cdot C + \mathcal{O}(U^2)$ into the second addend,

$$-\dot{U}\cdot(C\overline{\Sigma}C) = \dot{U}\cdot\overline{\Pi}_0\cdot U\cdot C + \mathcal{O}(U^2\dot{U}). \tag{92}$$

Together with the third addend, this can be integrated to the value of the mean-field-like (non-2PI) second order self-energy diagram $U\cdot\overline{\Pi}_0\cdot U\cdot C$, plus third order corrections. The fourth addend can be integrated to

$$\frac{1}{3}\sum_{\gamma_3}(U\cdot\overline{\Pi}_0\cdot U)_{\alpha_1\alpha_3\alpha'_3\alpha'_1}C_{\gamma_3}, \tag{93}$$

which is the value of the 2PI second order self-energy diagram. Thus, we recovered all diagrams up to second order, and the remaining $\mathcal{O}(U^2\dot{U})$ leads to some correction of $\mathcal{O}(U^3)$. The proof for the thermodynamic potential is similar.

6.3. Modified U-flow starting at mean-field theory

In Ref. [36], a slight modification of the U-flow is proposed which results in a different starting point of the flow, namely mean-field theory instead of the non-interacting problem. The modified U-flow is defined by

$$\Phi_\lambda(\text{modified } U\text{-flow}) = \Phi_\lambda(\text{plain } U\text{-flow}) + \frac{1}{2}G\cdot(U - U_\lambda)\cdot G, \tag{94}$$

where Φ_λ(plain U-flow) refers to the scheme described in Sect. 6.1. For an interpretation of the modified U-flow, consider the expansion of the Luttinger-Ward functional given in Eq. (20). In the plain U-flow, each U in this expansion is replaced by U_λ. In the modified U-flow, the first order contribution $\frac{1}{2}G\cdot U\cdot G$ is excluded from this replacement. At the starting point $U_{\lambda_\mathrm{i}} = 0$ of the flow, $\Phi_{\lambda_\mathrm{i}}$ in the modified scheme is given by precisely that first order contribution,

$$\Phi_{\lambda_\mathrm{i}} = \frac{1}{2}G\cdot U\cdot G, \qquad \Phi^{(1)}_{\lambda_\mathrm{i}} = -\Sigma_{\lambda_\mathrm{i}} = U\cdot G, \qquad \Phi^{(2)}_{\lambda_\mathrm{i}} = U, \qquad \Phi^{(n)}_{\lambda_\mathrm{i}} = 0,\ n \geq 3. \tag{95}$$

As $\Sigma = -U\cdot G$ is the Hartree-Fock self-consistency equation, we see that the flow starts at mean-field theory (cf. [27]). At the end point $U_{\lambda_\mathrm{f}} = U$ of the flow, the full genuine Luttinger-Ward functional is recovered. If required, the flow of the other functionals is derived from the flow of Φ_λ. The effective action is given by $\Gamma_\lambda = \Phi_\lambda + \Gamma_0$, and W_λ is obtained from Γ_λ by a Legendre transformation.

In the same spirit, one could define more general flow schemes that start at nth order self-consistent perturbation theory. In the definition of Φ_λ, the replacement $U \to U_\lambda$ would be applied only to contributions of order U^{n+1} and higher. Depending on the problem of interest, starting the flow with nth order self-consistent perturbation theory might or might not be advantageous; see the discussion of truncated C-flow for the anharmonic oscillator above and Ref. [51] for the single-impurity Anderson model.

In the framework of the modified scheme, the functional Φ(plain U-flow) does not play the role of the Luttinger-Ward functional. Therefore, we label it Ψ from now on such that Eq. (94) takes the form $\Phi_\lambda = \Psi_\lambda + \frac{1}{2} G \cdot (U - U_\lambda) \cdot G$. For the flow equation follows $\dot{\Phi} = \dot{\Psi} - \frac{1}{2} G \cdot \dot{U} \cdot G = \dot{\Psi} - \frac{1}{4} \operatorname{Tr} \dot{U} \cdot \Pi$. We insert $\dot{\Psi}$ from Eq. (77) and obtain

$$\dot{\Phi} = \frac{1}{3!} \operatorname{Tr} \dot{U} \cdot \left[\left(\Pi^{\mathrm{inv}} + \Psi^{(2)} \right)^{\mathrm{inv}} - \Pi \right], \tag{96}$$

$$\dot{\Phi}^{(1)}_{\gamma_1} = \frac{1}{3} \sum_{\gamma_2} \left[\left(I + \Psi^{(2)} \cdot \Pi \right)^{\mathrm{inv}} \cdot \dot{U} \cdot \left(I + \Pi \cdot \Psi^{(2)} \right)^{\mathrm{inv}} - \dot{U} \right]_{\alpha_1 \alpha_2 \alpha_2' \alpha_1'} G_{\gamma_2} + \mathcal{O}\left(\Psi^{(3)} \right), \tag{97}$$

where $\Psi^{(2)}_\lambda = \Phi^{(2)}_\lambda + U_\lambda - U$ and $\Psi^{(3)} = \Phi^{(3)}$. On the analogy of Eqs. (82) and (83) follows

$$\dot{\overline{\Phi}} = \overline{\dot{\Phi}} - \overline{\Phi}^{(1)} \cdot \left(\overline{\Pi}^{\mathrm{inv}} + \overline{\Phi}^{(2)} \right)^{\mathrm{inv}} \cdot \overline{\dot{\Phi}}^{(1)}, \qquad \dot{\overline{\Phi}}^{(1)} = \left(I + \overline{\Phi}^{(2)} \cdot \overline{\Pi} \right)^{\mathrm{inv}} \cdot \overline{\dot{\Phi}}^{(1)}. \tag{98}$$

As for the plain U-flow, the flow equation for the thermodynamic potential has the form $\dot{\overline{\Omega}} = \overline{\dot{\Phi}}/\beta$. The initial value is now the mean-field potential $\overline{\Omega}_{\mathrm{MF}}$ indicated in Eq. (43).

6.4. Truncation of the modified U-flow

In the modified U-flow, the lowest truncation of the hierarchy of flow equations that leads to a flowing self-energy $\overline{\Sigma}_\lambda = -\overline{\Phi}^{(1)}_\lambda$ is at level $m = 2$: set $\overline{\Phi}^{(2)}_\lambda = \overline{\Phi}^{(2)}_{\lambda_{\mathrm{i}}} = U$ and $\overline{\Phi}^{(n)}_\lambda = \overline{\Phi}^{(n)}_{\lambda_{\mathrm{i}}} = 0, n \geq 3$. The flow of the self-energy in this approximation is

$$\begin{aligned} \dot{\overline{\Sigma}}^{\lambda}_{\gamma_1} = & -\frac{1}{6} \sum_{\gamma_2, \gamma_3} \left(I + U \cdot \overline{\Pi}_\lambda \right)^{\mathrm{inv}}_{\gamma_1 \gamma_2} \\ & \times \left[\left(I + U_\lambda \cdot \overline{\Pi}_\lambda \right)^{\mathrm{inv}} \cdot \dot{U}_\lambda \cdot \left(I + \overline{\Pi}_\lambda \cdot U_\lambda \right)^{\mathrm{inv}} - \dot{U}_\lambda \right]_{\alpha_2 \alpha_3 \alpha_3' \alpha_2'} \overline{G}^{\lambda}_{\gamma_3}, \end{aligned} \tag{99}$$

where U_λ refers to the flow parameter dressed value of the interaction, while U denotes the bare one. The flow equation for the thermodynamic potential $\dot{\overline{\Omega}} = \overline{\dot{\Phi}}/\beta$ reads

$$\dot{\overline{\Omega}}_\lambda = \frac{1}{3!\beta} \operatorname{Tr} \dot{U}_\lambda \cdot \left[\left(\overline{\Pi}^{\mathrm{inv}}_\lambda + U_\lambda \right)^{\mathrm{inv}} - \overline{\Pi}_\lambda \right]. \tag{100}$$

It can be shown that the solutions of these approximate flow equations comprise all diagrams contributing to self-consistent Hartree-Fock (mean-field) and to second order perturbation theory with mean-field propagators,

$$\overline{\Sigma}_{\lambda_{\mathrm{f}}} = \overline{\Sigma}_{\mathrm{exact}} + \mathcal{O}\left(U^3 \overline{G}^5_{\mathrm{MF}} \right), \qquad \overline{\Omega}_{\lambda_{\mathrm{f}}} = \overline{\Omega}_{\mathrm{exact}} + \mathcal{O}\left(U^3 \overline{G}^6_{\mathrm{MF}} \right). \tag{101}$$

For the proof, we start from the initial condition $\overline{\Sigma}_{\lambda_{\mathrm{i}}} = \overline{\Sigma}_{\mathrm{MF}}$, $\overline{G}_{\lambda_{\mathrm{i}}} = \overline{G}_{\mathrm{MF}}$, $\overline{\Pi}_{\lambda_{\mathrm{i}}} = \overline{\Pi}_{\mathrm{MF}}$. From $\dot{\overline{\Sigma}} = \mathcal{O}\left(U \dot{U} \overline{G}^3 \right)$ follows $\overline{\Sigma}_\lambda = \overline{\Sigma}_{\mathrm{MF}} + \mathcal{O}\left(U^2 \overline{G}^3_{\mathrm{MF}} \right)$, hence $\overline{G}_\lambda = \overline{G}_{\mathrm{MF}} + \mathcal{O}\left(U^2 \overline{G}^5_{\mathrm{MF}} \right)$,

$\overline{\Pi}_\lambda = \overline{\Pi}_{\mathrm{MF}} + \mathcal{O}\big(U^2\overline{G}^6_{\mathrm{MF}}\big)$. Therefore,

$$\dot{\overline{\Sigma}}{}^\lambda_{\gamma_1} = \frac{1}{3}\sum_{\gamma_3}\Big(U_\lambda \cdot \overline{\Pi}_{\mathrm{MF}} \cdot \dot{U}_\lambda + \dot{U}_\lambda \cdot \overline{\Pi}_{\mathrm{MF}} \cdot U_\lambda\Big)_{\alpha_1\alpha_3\alpha_3'\alpha_1'} \overline{G}_{\mathrm{MF},\gamma_3} + \mathcal{O}\left(U^2\dot{U}\overline{G}^5_{\mathrm{MF}}\right). \quad (102)$$

Integration from λ_{i} to λ_{f} yields

$$\overline{\Sigma}_{\lambda_{\mathrm{f}}} = \overline{\Sigma}_{\mathrm{MF}} + \frac{1}{3}\sum_{\gamma_3}\big(U \cdot \overline{\Pi}_{\mathrm{MF}} \cdot U\big)_{\alpha_1\alpha_3\alpha_3'\alpha_1'} \overline{G}_{\mathrm{MF},\gamma_3} + \mathcal{O}\left(U^3\overline{G}^5_{\mathrm{MF}}\right). \quad (103)$$

The second addend on the right-hand-side is indeed the 2PI second order self-energy diagram with mean-field propagators. The proof for $\overline{\Omega}$ can be performed analogously.

6.5. Application to the anharmonic oscillator

For a practical application of plain and modified U-flow, we use Eq. (26) for the calculation of $\dot{\overline{G}}$. In plain U-flow, one obtains for the self-energy (still for general γ-indices)

$$\begin{aligned}\dot{\overline{\Sigma}}{}^\lambda_{\gamma_1} = & -\frac{1}{3}\sum_{\gamma_2}\left[\big(I + U_\lambda \cdot \overline{\Pi}_\lambda\big)^{\mathrm{inv}} \cdot \dot{U}_\lambda \cdot \big(I + \overline{\Pi}_\lambda \cdot U_\lambda\big)^{\mathrm{inv}} + \frac{\dot{U}_\lambda}{2}\right]_{\alpha_1\alpha_2\alpha_2'\alpha_1'} \overline{G}^\lambda_{\gamma_2} \\ & -\frac{1}{2}\sum_{\gamma_2} U_{\lambda,\gamma_1\gamma_2}\dot{\overline{G}}{}^\lambda_{\gamma_2}. \end{aligned} \quad (104)$$

Introducing the quantity $\overline{\Upsilon}_\lambda = I - \big(I + U_\lambda \cdot \overline{\Pi}_\lambda\big)^{\mathrm{inv}}$, one finds

$$\dot{\overline{\Sigma}}{}^\lambda_{\gamma_1} = -\frac{1}{3}\sum_{\gamma_2}\left[\left(\overline{\Upsilon}_\lambda \cdot \dot{U}_\lambda \cdot \overline{\Upsilon}^{\mathsf{T}}_\lambda - \overline{\Upsilon}_\lambda \cdot \dot{U}_\lambda - \dot{U}_\lambda \cdot \overline{\Upsilon}^{\mathsf{T}}_\lambda + \frac{3}{2}\dot{U}_\lambda\right)_{\alpha_1\alpha_2\alpha_2'\alpha_1'} \overline{G}^\lambda_{\gamma_2} + \frac{3}{2}U_{\lambda,\gamma_1\gamma_2}\dot{\overline{G}}{}^\lambda_{\gamma_2}\right], \quad (105)$$

$$\dot{\overline{\Omega}} = -\frac{1}{3!\beta}\operatorname{Tr}\dot{U}_\lambda \cdot \overline{\Pi}_\lambda \cdot \left[\overline{\Upsilon}_\lambda - \frac{3}{2}I\right]. \quad (106)$$

On the other hand, one finds in the modified U-flow that

$$\dot{\overline{\Sigma}}{}^\lambda_{\gamma_1} = -\frac{1}{3}\sum_{\gamma_2}\left[\overline{\Upsilon}_\lambda \cdot \dot{U}_\lambda \cdot \overline{\Upsilon}^{\mathsf{T}}_\lambda - \overline{\Upsilon}_\lambda \cdot \dot{U}_\lambda - \dot{U}_\lambda \cdot \overline{\Upsilon}^{\mathsf{T}}_\lambda\right]_{\alpha_1\alpha_2\alpha_2'\alpha_1'} \overline{G}^\lambda_{\gamma_2} - \frac{1}{2}\sum_{\gamma_2} U_{\gamma_1\gamma_2}\dot{\overline{G}}{}^\lambda_{\gamma_2}, \quad (107)$$

$$\dot{\overline{\Omega}} = -\frac{1}{3!\beta}\operatorname{Tr}\dot{U}_\lambda \cdot \overline{\Pi}_\lambda \cdot \overline{\Upsilon}_\lambda. \quad (108)$$

Note that due to $(\overline{\Upsilon}^{\mathsf{T}}_\lambda)_{\gamma_1,\gamma_2} = \overline{\Upsilon}_{\lambda;\gamma_2,\gamma_1}$, all occurrences of $\overline{\Upsilon}^{\mathsf{T}}$ can generally be replaced by $\overline{\Upsilon}$. This shall be done below.

Now, we again consider the specific problem of the anharmonic oscillator [i.e. $\zeta = +1$, $\gamma = (\tau, \tau')$]. The above equations shall be Fourier transformed according to Eqs. (50) and (51). Note that $\overline{\Upsilon}^{(\mathsf{T})}_\lambda$ is neither propagator nor vertex but rather $\sim I$. Suitable Fourier transformation definitions are

$$\overline{\Upsilon}_{n_1n_1'n_2n_2'} = \int_{\tau_1}\cdots\int_{\tau_2'} e^{+i\omega_{n_1}\tau_1 + i\omega_{n_1'}\tau_1' - i\omega_{n_2}\tau_2 - i\omega_{n_2'}\tau_2'}\,\overline{\Upsilon}(\tau_1, \tau_1', \tau_2, \tau_2'), \quad (109)$$

$$\overline{\Upsilon}^{\mathsf{T}}_{n_1n_1'n_2n_2'} = \int_{\tau_1}\cdots\int_{\tau_2'} e^{-i\omega_{n_1}\tau_1 - i\omega_{n_1'}\tau_1' + i\omega_{n_2}\tau_2 + i\omega_{n_2'}\tau_2'}\,\overline{\Upsilon}^{\mathsf{T}}(\tau_1, \tau_1', \tau_2, \tau_2'). \quad (110)$$

Let us specify the flow parameter dependence of U_λ via a function $f_\lambda \in \mathbb{R}$ with $f_{\lambda_{\mathrm{i}}} = 0$ and $f_{\lambda_{\mathrm{f}}} = 1$ such that

$$U_\lambda(\tau_1, \tau_1', \tau_2, \tau_2') = f_\lambda g \delta(\tau_1 = \tau_1' = \tau_2 = \tau_2'). \quad (111)$$

In practical calculations, $f_\lambda = \lambda$ with $\lambda_{\mathrm{i}} = 0$ and $\lambda_{\mathrm{f}} = 1$ is used. The choice of U_λ makes it possible to show that

$$\overline{\Upsilon}_{\lambda;n_1n_1'n_2} = \left[1 + \frac{f_\lambda g}{2\beta} \sum_n \overline{G}^\lambda_{-n} \overline{G}^\lambda_{n-n_1-n_1'}\right]^{-1} f_\lambda g \overline{G}^\lambda_{-n_2} \overline{G}^\lambda_{n_2-n_1-n_1'}, \tag{112}$$

$$\overline{\Upsilon}^{\intercal}_{\lambda;n_1n_1'n_2} = f_\lambda g \overline{G}^\lambda_{n_1} \overline{G}^\lambda_{n_1'} \left[1 + \frac{f_\lambda g}{2\beta} \sum_n \overline{G}^\lambda_n \overline{G}^\lambda_{n_1+n_1'-n}\right]^{-1}. \tag{113}$$

As expected from $(\overline{\Upsilon}^{\intercal}_\lambda)_{\gamma_1,\gamma_2} = \overline{\Upsilon}_{\lambda;\gamma_2,\gamma_1}$, one finds $\overline{\Upsilon}^{\intercal}_{\lambda;n_2,n_1+n_1'-n_2,n_1} = \overline{\Upsilon}_{\lambda;n_1,n_1',n_2}$. From now on, we will only use $\overline{\Upsilon}_\lambda$. It turns out that the third index of $\overline{\Upsilon}_\lambda$ is always summed over independently. This sum depends only on the sum of the first to indices. Thus, we introduce the definitions

$$\widetilde{\Upsilon}_{\lambda;n_1+n_1'} = \frac{1}{\beta} \sum_{n_2} \overline{\Upsilon}_{\lambda;n_1n_1'n_2} = \left[1 + \frac{f_\lambda g}{2} \left(\overline{GG}\right)_{n_1+n_1'}\right]^{-1} f_\lambda g \left(\overline{GG}\right)_{n_1+n_1'}, \tag{114}$$

$$\left(\overline{GG}\right)_N = \frac{1}{\beta} \sum_n \overline{G}_{-n} \overline{G}_{n-N}. \tag{115}$$

With these findings, the flow equations in plain U-flow become

$$\dot{\overline{\Omega}}_\lambda = -\frac{\dot{f}_\lambda g}{4!\beta^2} \sum_{n_1n_2} \overline{G}^\lambda_{n_1-n_2} \overline{G}^\lambda_{n_2} \widetilde{\Upsilon}_{\lambda;n_1} + \frac{\dot{f}_\lambda g}{8} \left(\frac{1}{\beta} \sum_n \overline{G}^\lambda_n\right)^2, \tag{116}$$

$$\dot{\overline{\Sigma}}^\lambda_{n_1} = -\frac{\dot{f}_\lambda g}{12\beta} \sum_n \widetilde{\Upsilon}^2_{\lambda;n} \overline{G}^\lambda_{n-n_1} + \frac{\dot{f}_\lambda g}{3\beta} \sum_n \widetilde{\Upsilon}_{\lambda;n} \overline{G}^\lambda_{n-n_1} - \frac{\dot{f}_\lambda g}{2\beta} \sum_n \overline{G}^\lambda_n - \frac{f_\lambda g}{2\beta} \sum_n \dot{\overline{G}}^\lambda_n. \tag{117}$$

The last addend in the second equation depends on $\dot{\overline{\Sigma}}^\lambda_n$ and makes the equation a self-consistent one. However, this self-consistency problem can be solved explicitly as the addend does not depend on n_1 (i.e. it is constant with respect to the external frequency). With the ansatz $\dot{\overline{\Sigma}}^\lambda_{n_1} = \overline{D}^\lambda_{n_1} + \overline{C}^\lambda$ where $\overline{D}^\lambda_{n_1}$ denotes the first three addends and $\overline{C}^\lambda$ the last addend, one finds:

$$\overline{C}^\lambda = -\left[1 + \frac{f_\lambda g}{2\beta} \sum_{n_2} \left(\overline{G}^\lambda_{n_2}\right)^2\right]^{-1} \frac{f_\lambda g}{2\beta} \sum_{n_2} \left(\overline{G}^\lambda_{n_2}\right)^2 \overline{D}^\lambda_{-n_2}, \tag{118}$$

With the same ansatz $\dot{\overline{\Sigma}}^\lambda_{n_1} = \overline{D}^\lambda_{n_1} + \overline{C}^\lambda$, one finds for the modified U-flow:

$$\dot{\overline{\Omega}}_\lambda = -\frac{\dot{f}_\lambda g}{4!\beta^2} \sum_{n_1n_2} \widetilde{\Upsilon}_{\lambda;n_1} \overline{G}^\lambda_{n_1-n_2} \overline{G}^\lambda_{n_2}, \tag{119}$$

$$\overline{D}^\lambda_{n_1} = -\frac{\dot{f}_\lambda g}{12\beta} \sum_n \widetilde{\Upsilon}^2_{\lambda;n} \overline{G}^\lambda_{n-n_1} + \frac{\dot{f}_\lambda g}{3\beta} \sum_n \widetilde{\Upsilon}_{\lambda;n} \overline{G}^\lambda_{n-n_1}, \tag{120}$$

$$\overline{C}^\lambda = -\left[1 + \frac{g}{2\beta} \sum_{n_2} \left(\overline{G}^\lambda_{n_2}\right)^2\right]^{-1} \frac{g}{2\beta} \sum_{n_2} \left(\overline{G}^\lambda_{n_2}\right)^2 \overline{D}^\lambda_{-n_2}. \tag{121}$$

In both schemes, a non-trivial frequency dependence is generated in the self-energy in these lowest-order truncations (typically, this is different in 1PI fRG schemes). Note that the following symmetries hold: $\overline{G}_n = \overline{G}_{-n}$, $\left(\overline{GG}\right)_N = \left(\overline{GG}\right)_{-N}$, $\widetilde{\Upsilon}_N = \widetilde{\Upsilon}_{-N}$ and $\overline{D}_n = \overline{D}_{-n}$.

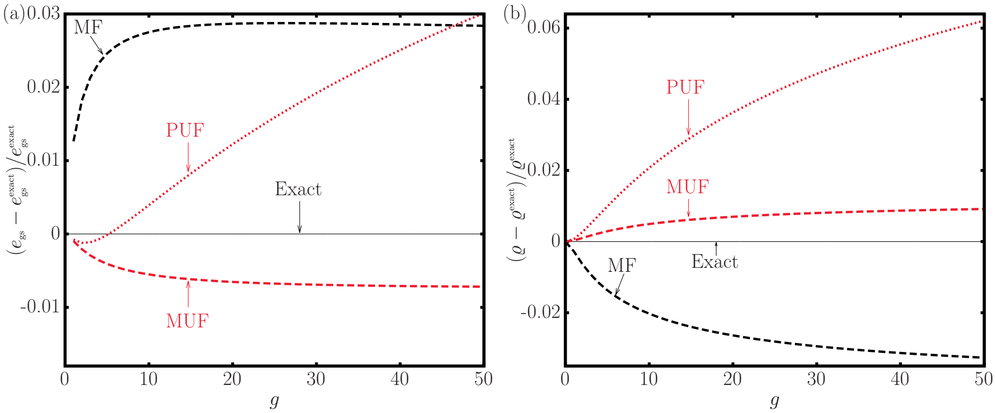

Figure 3. Numerical results for (a) the ground state energy and (b) the density as a function of the anharmonicity g. The relative difference to the exact results is shown. The lines present results obtained with the plain U-flow (dotted; PUF) and the modified U-flow (light [red] dashed; MUF). The U-flow data is calculated with $m_{\rm len} = 180$. The mean-field (MF) data are given for comparison.

Now, the $\beta \to \infty$ (i.e. $T \to 0$) limit can be performed. Then, the initial conditions in plain U-flow are

$$\overline{\Omega}_{\lambda_{\rm i}} = \frac{\omega_{\rm G}}{2}, \qquad \overline{\Sigma}_{\lambda_{\rm i}}(\nu) = 0. \tag{122}$$

The initial conditions in modified U-flow are

$$\overline{\Omega}_{\lambda_{\rm i}} = \frac{1}{2}\sqrt{\omega_{\rm G}^2 + \overline{\Sigma}_{\rm MF}} - \frac{1}{2g}\overline{\Sigma}_{\rm MF}^2, \qquad \overline{\Sigma}_{\lambda_{\rm i}}(\nu) = \overline{\Sigma}_{\rm MF} = \frac{g}{4}\frac{1}{\sqrt{\omega_{\rm G}^2 + \overline{\Sigma}_{\rm MF}}}. \tag{123}$$

6.6. Numerical results for the anharmonic oscillator

We implemented the zero temperature U-flow equations making use of the non-uniform frequency grid introduced in Appendix A. In both schemes, the number of equations scales $\sim m_{\rm len}$ and the effort for computing the right-hand-side is also $\sim m_{\rm len}$; the effort for the calculation of the set of differential equations in each step of the flow is thus $\sim m_{\rm len}^2$ (like in regular C-flow at truncation order $m = 4$). Reaching numerical convergence with respect to $m_{\rm len}$ is thus not an issue as it can be tuned to rather large values. Fig. 3 shows converged numerical data for $m_{\rm len} = 180$.

The modified U-flow curve is a lot closer to the exact result than the plain U-flow curve. In fact, it reproduces the exact results within 1% and can thus compete with the internally closed C-flow method. Recall, however, that the effort to calculate the set of differential equations in each step of the flow scales $\sim m_{\rm len}^2$ in the modified U-flow while it scales $\sim m_{\rm len}^4$ in the internally closed C-flow. There is an intuitive reason for the success of the modified U-flow: the initial condition corresponds to the Hartree-Fock approximation which reproduces the exact results quite well already ($< 3\%$). Thus, much of the interacting physics is captured initially and the flow only has to take care of the missing part. Apparently, starting the flow from the non-interacting system is a significantly more unfavourable initial condition which explains the less successful results of plain U-flow. This difference between the U-flow schemes can also be understood from the respective discussions of the degree of perturbation theory contained: Both schemes comprise second order perturbation theory but plain U-flow does so with the bare propagator while modified U-flow does so with the mean-field propagator.

7. DFT-fRG

A method similar to U-flow was proposed in Refs. [44, 45] and applied to the quantum anharmonic oscillator in Ref. [46]. Instead of working with an external source depending on two indices [like in Eq. (9)], a purely diagonal one $J_{\alpha_1\alpha_2} = \delta_{\alpha_1\alpha_2} J_{\alpha_1}$ is introduced. Thus, the formal starting point of the considerations is not a 2PI functional but rather a two-particle point-irreducible ("2PPI") one. This term is introduced in Ref. [52] with the following descriptive explanation: a 2PPI diagram is a 1PI diagram that cannot be split into two by cutting two internal lines attached to the same vertex. This implies differences in the derivation of the flow equations and in their structure. In particular, it turns out that the Luttinger-Ward functional cannot be computed reasonably because the relation $G = -\frac{\delta W}{\delta J}$ cannot be solved explicitly for J any more. The manifest remaining option is to work with the functional Γ and its moments. Furthermore, the diagonality of J causes G to be the density of the physical system. According to the discussion of Sect. 4.4 the ground state energy can be expressed through the functional $\Gamma[G]$. Therefore, one works with an energy functional that depends on the density. This brings about a close relation to density functional theory [53] (in the plain Hohenberg-Kohn sense) and motivates us to use the term DFT-fRG. The physical state indicated by a bar $\overline{}$ is defined as above, namely by the minimum of the energy functional. Thus, this method yields the minimum of the energy and the corresponding density of the interacting system at the end of the flow. In this sense, DFT-fRG is a way of conducting density functional theory calculations alternative to the Kohn-Sham idea [53]. Truncated DFT-fRG can even be used to derive an approximation to the energy functional $\Gamma[G]$ of the interacting system. It remains to be seen if this approximation—which has the structure of a Taylor expansion around the ground state density, see below—leads to useful results for fermionic many-body problems.

Introducing the flow parameter simply via $U \to \lambda U$, $\lambda_\mathrm{i} = 0$ and $\lambda_\mathrm{f} = 1$, flow equations can be derived for $\overline{\Gamma}^{(n)}$ without further conceptual complications. However, the initial conditions $\overline{\Gamma}^{(n)}_{\lambda_\mathrm{i}}$ are rather lengthy to compute because even for the non-interacting case Γ takes a non-trivial form (in contrast to Φ). The explicit calculations can be found in Ref. [46]; note that in that work the moments $\overline{\Gamma}^{(n)}$ are not defined as functional derivatives but rather only implicitly [namely via Eq. (14) of that work]. Thus, the $\overline{\Gamma}^{(n)}$ cannot be expected to obey all the index permutation symmetries that functional derivatives would have.[+]

Once the flow equations $\dot{\overline{\Gamma}}^{(n)}_{\lambda}$ and the initial conditions $\overline{\Gamma}^{(n)}_{\lambda_\mathrm{i}}$ are determined, a natural truncation is obtained by setting $\overline{\Gamma}^{(n)}_{\lambda} = \overline{\Gamma}^{(n)}_{\lambda_\mathrm{i}}$ for all $n \geq m$ for a certain m. This is again motivated from a weak coupling perspective (cf. Sect. 4.2). At the end of the flow, one obtains an approximation to the interacting $\overline{\Gamma}^{(n)}_{\lambda}$ for $n < m$. Along with the non-interacting $\overline{\Gamma}^{(n)}_{\lambda}$ for $n \geq m$, these moments constitute an approximation to the energy functional which is valid "locally" around its minimum. In this way, DFT-fRG is able to provide an approximation to the interacting energy functional.

[+] This implicit definition was dealt with consistently in Ref. [46] but the reader should keep it in mind in order to avoid confusion.

We here specify the (first three) flow equations for the quantum anharmonic oscillator. For a self-contained presentation we stick to the notation introduced above up to a redefinition of $\overline{G}_\lambda$ including a factor $\frac{1}{\beta}$ (compare to Ref. [46]). From $\dot{\overline{\Gamma}}{}^{(1)}_\lambda = 0$, one obtains a flow equation for $\overline{G}_\lambda$. Instead of providing a flow equation for $\overline{\Gamma}{}^{(2)}_\lambda$, it is equivalently given for $\overline{W}{}^{(2)}_\lambda$. Adopting the definition for $\overline{\Gamma}{}^{(n)}$ by functional derivatives and additionally performing the zero temperature limit (this implies some minor differences to the equations given in Ref. [46]), one finds

$$\dot{\overline{\Omega}}_\lambda = \frac{g}{24}\left[\overline{G}{}^2_\lambda + \int_0^\infty \frac{d\nu_1}{\pi}\overline{W}{}^{(2)}_\lambda(\nu_1)\right], \tag{124}$$

$$\dot{\overline{G}}_\lambda = \frac{g}{12}\overline{W}{}^{(2)}_\lambda(0)\left[-\overline{G}_\lambda + \int_0^\infty \frac{d\nu_1}{2\pi}\left(\overline{W}{}^{(2)}(\nu_1)\right)^2 \overline{\Gamma}{}^{(3)}_\lambda(\nu_1,-\nu_1)\right], \tag{125}$$

$$\begin{aligned}\dot{\overline{W}}{}^{(2)}_\lambda(\nu) = -\frac{g}{12}\overline{W}{}^{(2)}_\lambda(\nu)^2\Bigg\{1 + \frac{12}{g}\dot{\overline{G}}_\lambda\overline{\Gamma}{}^{(3)}_\lambda(0,\nu) - \int_0^\infty \frac{d\nu_1}{2\pi}\overline{W}{}^{(2)}_\lambda(\nu_1)^2\,\overline{\Gamma}{}^{(4)}_\lambda(\nu_1,-\nu_1,\nu) \\ + \int_0^\infty \frac{d\nu_1}{2\pi}\overline{W}{}^{(2)}_\lambda(\nu_1)^2\left[\overline{W}{}^{(2)}_\lambda(\nu_1+\nu)\left(\overline{\Gamma}{}^{(3)}_\lambda(\nu_1,\nu)\right)^2 + \overline{W}{}^{(2)}_\lambda(\nu_1-\nu)\left(\overline{\Gamma}{}^{(3)}_\lambda(\nu_1,\nu)\right)^2\right]\Bigg\}.\end{aligned} \tag{126}$$

The initial conditions are

$$\overline{\Omega}_0 = \frac{\omega_\mathrm{G}}{2}, \qquad \overline{G}_0 = \frac{1}{2\omega_\mathrm{G}}, \qquad \overline{W}{}^{(2)}_\lambda(\nu) = \frac{2}{\omega_\mathrm{G}}\frac{1}{\nu^2+4\omega_\mathrm{G}^2}, \tag{127}$$

$$\overline{\Gamma}{}^{(3)}_0(\nu_1,\nu_2) = -\omega_\mathrm{G}^2\left(\nu_1^2+\nu_1\nu_2+\nu_2^2+12\omega_\mathrm{G}^2\right), \tag{128}$$

$$\begin{aligned}\overline{\Gamma}{}^{(4)}_\lambda(\nu_1,\nu_2,\nu_3) = \Bigg[2\omega_\mathrm{G}^3\frac{\left((\nu_1+\nu_2)^2+(\nu_1+\nu_2)\,\nu_3+\nu_3^2+12\omega_\mathrm{G}^2\right)\left(\nu_1^2+\nu_1\nu_2+\nu_2^2+12\omega_\mathrm{G}^2\right)}{(\nu_1+\nu_2)^2+4\omega_\mathrm{G}^2} \\ - \frac{\omega_\mathrm{G}^3 f(\nu_1,\nu_2,\nu_3)}{\left((\nu_1+\nu_2)^2+4\omega_\mathrm{G}^2\right)\left((\nu_2+\nu_3)^2+4\omega_\mathrm{G}^2\right)}\Bigg] \\ + (\nu_1\to\nu_2\to\nu_3\to\nu_1) + (\nu_1\to\nu_3\to\nu_2\to\nu_1),\end{aligned} \tag{129}$$

with

$$\begin{aligned}f(\nu_1,\nu_2,\nu_3) = {} & 640\omega_\mathrm{G}^6 + 48\omega_\mathrm{G}^4\left[3\nu_1^2+4\nu_2^2+3\nu_3^2+4\nu_1\nu_2+2\nu_1\nu_3+4\nu_2\nu_3\right] \\ & +4\omega_\mathrm{G}^2\big[3\nu_1^4+2\nu_2^4+4\nu_2^3\nu_3+10\nu_2^2\nu_3^2+8\nu_2\nu_3^3+3\nu_3^4+4\nu_1^3\left(2\nu_2+\nu_3\right) \\ & \qquad +2\nu_1\left(2\nu_2+\nu_3\right)\left(\nu_2^2+\nu_2\nu_3+2\nu_3^2\right)+2\nu_1^2\left(5\nu_2^2+5\nu_2\nu_3+2\nu_3^2\right)\big] \\ & +\nu_2^2\nu_3^2\left(\nu_2+\nu_3\right)^2+\nu_1\nu_2\nu_3^2\left(\nu_2+\nu_3\right)\left(2\nu_2+\nu_3\right) \\ & +\nu_1^2\left(\nu_2^4+2\nu_2^3\nu_3+6\nu_2^2\nu_3^2+5\nu_2\nu_3^3+\nu_3^4\right) \\ & +\nu_1^3\left(2\nu_2+\nu_3\right)\left(\nu_2^2+\nu_2\nu_3+2\nu_3^2\right)+\nu_1^4\left(\nu_2^2+\nu_2\nu_3+\nu_3^2\right).\end{aligned} \tag{130}$$

It is a generic feature of the 2PPI approach that, due to the diagonality of the external source J, $\overline{G}$ is not frequency dependent; this is neither due to the simplicity of the model of the oscillator nor to the truncation. Also, $\overline{W}{}^{(2)}$ depends on only one frequency (instead of three as it would in a 2PI approach). This is a clear advantage in the numerical treatment of the problem if indeed only the accessible diagonal quantities are desired.

Three truncation schemes are investigated in Ref. [46]. The natural one is obtained by setting $\overline{\Gamma}^{(n)}_{\lambda}$ to their initial values $\overline{\Gamma}^{(n)}_{\lambda_\mathrm{i}}$ for $n \geq 3$. A reduced scheme is defined by setting $\overline{\Gamma}^{(3),(4)}_{\lambda}$ to zero. This reduction allows to gain some analytical insights and solve the flow equations analytically [46]

$$e_\mathrm{gs} = \omega_\mathrm{G} \left(\frac{1}{4} \frac{g/4!}{1+g/4!} + \sqrt{1+g/4!} - 1 \right), \qquad \varrho = \frac{1}{2\omega_\mathrm{G}} \frac{1}{1+g/4!}. \tag{131}$$

A physically motivated suggestion also leads to an improved scheme [46]: At $\lambda = \lambda_\mathrm{i}$, the relation $\overline{G}_{\lambda_\mathrm{i}} = \frac{1}{2\omega_\mathrm{G}}$ holds. For $\lambda \neq \lambda_\mathrm{i}$, this relation is inverted to define an effective λ-dependent frequency characterizing the oscillator $\omega^\mathrm{eff}_\lambda = \frac{1}{2\overline{G}_\lambda}$. This $\omega^\mathrm{eff}_\lambda$ is then used to calculate $\overline{\Gamma}^{(3),(4)}_{\lambda}$ according to

$$\overline{\Gamma}^{(3),(4)}_{\lambda} = \overline{\Gamma}^{(3),(4)}_{\lambda_\mathrm{i}} \Big|_{\omega_\mathrm{G} \to \omega^\mathrm{eff}_\lambda}. \tag{132}$$

Even without performing explicit calculations, one can state two points: on the one hand, the motivation for this ad-hoc replacement is physically comprehensible: it corresponds to finding the harmonic oscillator that reproduces the present density at the given RG scale λ. In a sense, this is similar to the mean-field idea. On the other hand, the replacement is unsystematic and carries the danger of double counting of diagrams. Whether this is indeed the case, remains to be investigated. Such a study is technically not straightforward to conduct and we refrain from pursuing it here.

Numerical results for the quantum anharmonic oscillator were presented in Ref. [46] for finite temperatures $T > 0$. Our data for the reduced and improved DFT-fRG truncation schemes differ from the ones given there.* As for the other fRG schemes, we here only show temperature $T = 0$ curves. We numerically solved the DFT-fRG flow equations using the frequency grid introduced in Appendix A (the reduced scheme has of course an analytical solution). The number of flow equations scales $\sim m_\mathrm{len}$ in the natural as well as in the improved scheme. Taking into account the integrations on the right-hand-sides, the effort to calculate the set of differential equations in each step of the flow scales $\sim m^2_\mathrm{len}$. Results for all three truncation schemes are shown in Fig. 4. Note that the main plots show the ground state energy and the density as a function of g (and not the relative difference to the exact result as above). This is because the reduced and natural DFT-fRG curves are rather far off from the exact curve compared to the other RG approaches discussed here. Even for this simple problem of the oscillator, these two methods are found to perform much worse than simple mean-field theory. In contrast, the improved scheme reproduces the exact curve very well. This is discussed in more depth below.

8. Comparison of the 2PI schemes and conclusion

In this section, the anharmonic oscillator results obtained from the most successful schemes introduced above shall be compared to one another, namely the internally closed C-flow, modified U-flow and improved DFT-fRG. Moreover, they shall be set into context by comparing them to results of two 1PI fRG schemes [4]. These two

---

* The first discrepancy is that the free energy curve in the reduced scheme shown in Figure 6 of Ref. [46] does not agree with the provided analytical result. The second point involves the numerical data for the free energy and density calculated in the improved DFT-fRG scheme shown in Figures 6 and 7 of Ref. [46]. The authors of Ref. [46] informed us that a mistake in their numerical implementation is the only origin of the discrepancy to our results.

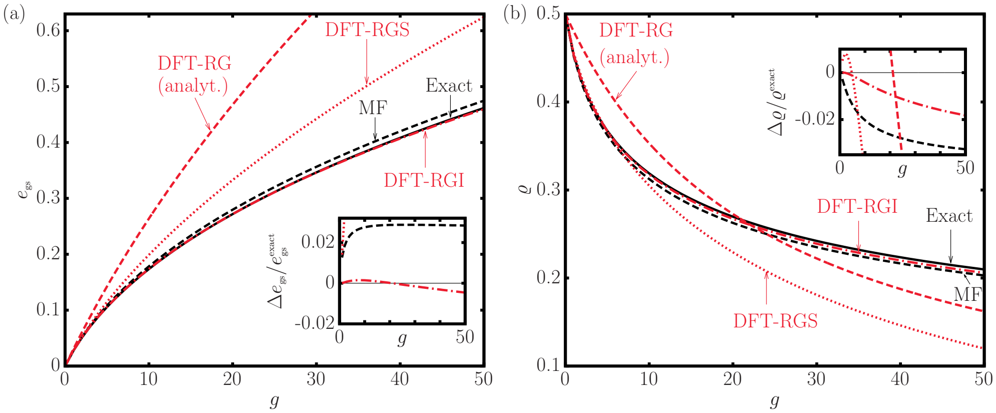

Figure 4. Numerical results for (a) the ground state energy and (b) the density as a function of the anharmonicity g. Note that this time the main plots show the absolute curves, while the insets show the relative difference to the exact curve. We label the schemes by the same names that were used in Ref. [46] for better comparability. The natural truncation (DFT-RGS) and improved DFT-fRG (DFT-RGI) data are calculated with $m_{\rm len} = 180$. For comparison, the exact, mean-field (MF) and analytical reduced DFT-fRG (DFT-RG) curves are plotted also.

schemes are based on vertex expansion and can be applied to the fermionic many-body problem (cf. Sect. 2) in a straight-forward manner - this is in contrast to fRG schemes based on potential expansion. We additionally give brief accounts of the general advantages and drawbacks of the different schemes and on the prospects of applying 2PI fRG to zero- and one-dimensional fermionic quantum many-body problems.

The first 1PI approach to compare with is the regular Matsubara fRG scheme that is obtained by truncating the set of flow equations at second order. The second is the modification of the first suggested by Katanin [30]—it corresponds to replacing the so called single-scale propagator with a full λ-derivative of the full propagator in the flow equation for the two-particle vertex. The number of flow equations scales $\sim m_{\rm len}^3$ in both 1PI fRG schemes. Both schemes use a sharp imaginary frequency cutoff as flow parameter. This means that the integrations on the right-hand-sides of the flow equations are "canceled" by a δ-function in the regular 1PI fRG whereas this is not entirely the case in Katanin 1PI fRG. Consequently, the effort to calculate the set of differential equations in each step of the flow scales $\sim m_{\rm len}^3$ in regular 1PI fRG and $\sim m_{\rm len}^4$ in Katanin 1PI fRG. For the ground state energy and the density of the anharmonic oscillator, the original numerical 1PI fRG results [4] are used for comparison to the 2P(P)I schemes.

Fig. 5 shows the numerical results. First of all, all three 2P(P)I schemes outperform the 1PI ones (except for improved DFT-fRG in the case of the density for $g \gtrsim 20$). That being said, internally closed C-flow and modified U-flow yield results similar to those of Katanin 1PI fRG (but a little better). One should stress, however, that modified U-flow does so with an effort $\sim m_{\rm len}^2$ in each step of the flow while the other two methods scale $\sim m_{\rm len}^4$. We emphasize that these scaling properties also hold for fermionic many-body problems.

As far as the ground state energy is concerned, improved DFT-fRG produces the most accurate results for the shown anharmonicities g. Note however, that similar

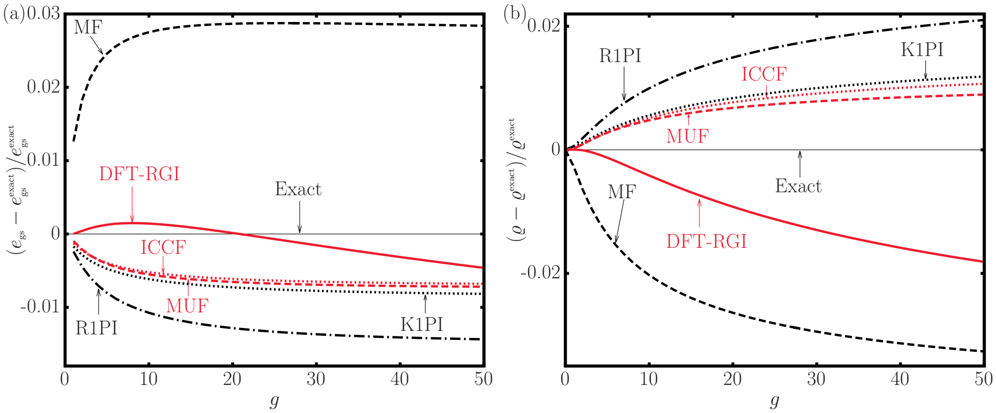

Figure 5. In this figure, the numerical results of the most successful 2PI methods for the ground state energy $e_{\rm gs}$ (a) and the density ϱ (b) are compared. The relative difference to the exact results is shown. Also, the mean-field (MF) curve and the regular 1PI fRG (R1PI) and Katanin 1PI fRG (K1PI) curves are presented. Internally closed C-flow (ICCF) is calculated at $m_{\rm len} = 45$, modified U-flow (MUF) and improved DFT-fRG (DFT-RGI) are calculated at $m_{\rm len} = 180$.

to what is observed for the density around $g = 20$, the improved DFT-fRG energy presumably becomes less accurate than the 1PI and 2PI ones around $g \approx 60$. This is strongly linked to the observation that in contrast to the other schemes discussed in this section the improved DFT-fRG results for the energy and density deviate in a non-monotonic way from the exact one. This behavior might originate from the ad hoc replacement $\omega_{\rm G} \to \omega_\lambda^{\rm eff}$. This mean-field-like substitution is at the same time at the heart of the success of the improved DFT-fRG scheme. This is plausible for the quantum anharmonic oscillator, as mean-field produces rather good results for this problem (see above). We expect that the improved DFT-fRG scheme is particularly suitable for problems in which the mean-field approximation already captures crucial parts of the interaction. In DFT-fRG it is generally impossible to access off-diagonal elements of two-point functions. This means that time-non-local properties of propagators cannot be computed although they are needed for the computation of certain observables (e.g. a spectral function). While this is true in equilibrium, time-non-local properties play an even more important role in non-equilibrium situations. Thus, it is not conceivable how to investigate non-equilibrium with this scheme. We re-emphasize that improved DFT-fRG might be prone to double counting of diagrammatic contributions. Prior to any application to fermionic many-body problems this issue should be thoroughly investigated.

Also the success of the modified U-flow with the Hartree-Fock solution as the starting point of the RG procedure heavily relies on the accuracy of mean-field theory for the problem at hand. When applied to zero- (quantum dots/impurities) or one-dimensional (quantum wires) fermionic many-body problems, modified U-flow faces the problem that the unrestricted Hartree-Fock starting point shows spurious symmetry breaking. This raises the interesting question whether the RG procedure can restore the symmetry that is broken in the initial conditions. If so, this approximation might turn out to be a favorable combination of the aspects of the physics mean-field gets right and those which other fRG schemes (such as e.g. 1PI fRG [4, 6, 1]) capture.

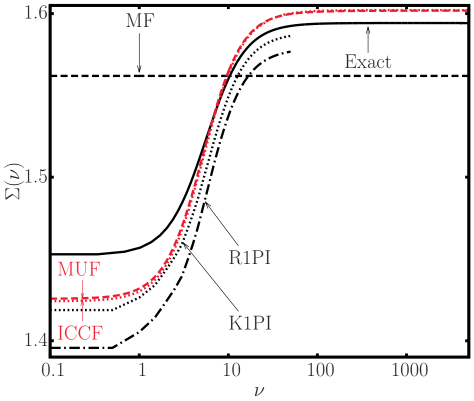

Figure 6. This figure shows the frequency dependence of the self-energy (on a log-linear scale) for several approximate methods at zero temperature and for coupling constant $g = 10$—improved DFT-fRG is missing as the self-energy cannot reasonably be computed in that scheme. Internally closed C-flow (ICCF) is calculated at $m_{\text{len}} = 45$ and modified U-flow (MUF) is calculated at $m_{\text{len}} = 180$.

In case the symmetry is not restored by the RG flow, one might resort to restricted Hartree-Fock as the starting point or employ plain U-flow for which the effort scales $\sim m_{\text{len}}^2$ in each step of the flow as well. The internally closed C-flow produces rather good results but does not constitute a true advance compared to Katanin 1PI fRG as it also scales $\sim m_{\text{len}}^4$ in each step of the flow.

As a last point, the frequency dependence of the self-energy of the anharmonic oscillator shall be discussed. Investigating this quantity promises some deeper understanding of the $e_{\text{gs}}(g)$ and $\varrho(g)$ curves. The frequency dependence for fixed interaction $g = 10$ is shown in Fig. 6.♯ All frequency dependent fRG schemes underestimate $\Sigma(\nu)$ around $\nu = 0$; in this regime, the 2PI fRG curves are closer to the exact solution. Recall that reproducing the correct behavior for small frequencies is more crucial than for large frequencies because $\Sigma(\nu)$ appears in the calculation of the propagator in sum with ν^2 such that the large ν contribution of $\Sigma(\nu)$ becomes less important. Thus, this observation makes it plausible that the 2PI schemes perform better than the 1PI ones.

Acknowledgements

We are grateful to Sandra Kemler and Jens Braun for numerous discussions. We thank the DFG for support via the Research Training Group 1995 "Quantum many-body methods in condensed matter systems".

♯ As curves for the frequency dependence of the self-energy were not shown in the original work Ref. [4] for regular and Katanin 1PI fRG, these curves were calculated within the scope of the present one using the code of Ref. [4]. An equidistant grid with $\Delta\nu = 0.5$ and $m_{\text{len}} = 100$ was employed.

Appendix

Appendix A. Numerical implementation

In our numerical calculations, we set $\omega_{\mathrm{G}} = 1$. The greatest challenge in implementing the zero temperature equations is that the frequency axes are continuous and must be discretized for the implementation: $\nu \to \nu_n$ (here, $-m_{\mathrm{len}} \leq n \leq m_{\mathrm{len}}$ denotes the discretization and not the Matsubara index). We require $\nu_{-n} = -\nu_n$. A cubic spline interpolator is used to interpolate function values at $\nu \notin \{\nu_n| - m_{\mathrm{len}} \leq n \leq m_{\mathrm{len}}\}$ and to calculate frequency integrals. Almost all right-hand-sides are $\mathcal{O}(\nu_{m_{\mathrm{len}}}^{-3})$, so that $\nu_{m_{\mathrm{len}}} \approx 5000$ is sufficient to match the accuracy of the differential equation solver. Furthermore, it seems advantageous to concentrate the frequencies around zero.

The following grid definition matches the above criteria (let $n \geq 0$):

$$\nu_n = \begin{cases} n\Delta\nu & \text{for } n \leq m_{\mathrm{len},1} \\ g_1 + \frac{f_1^{n-m_{\mathrm{len},1}}-1}{f_1-1}\Delta\nu & \text{for } m_{\mathrm{len},1} < n \leq m_{\mathrm{len},2} \\ g_2 f_2^{n-m_{\mathrm{len},2}} & \text{for } m_{\mathrm{len},2} < n \leq m_{\mathrm{len}} \end{cases} . \tag{A.1}$$

Here, g_1, g_2 are externally given parameters. $\Delta\nu = g_1/m_{\mathrm{len},1}$ where integer division defines $m_{\mathrm{len},1} = m_{\mathrm{len}}/3$ and $m_{\mathrm{len},2} = (2m_{\mathrm{len}})/3$. f_1 is determined such that $\nu_{m_{\mathrm{len},2}} = g_2$ and f_2 is determined such that $\nu_{m_{\mathrm{len}}} = 5120$. Preliminary calculations showed that $g_1 = 2$ and $g_2 = 20$ are reasonable choices. Numerical convergence with respect to m_{len} was checked carefully.

References

[1] Walter Metzner, Manfred Salmhofer, Carsten Honerkamp, Volker Meden, and Kurt Schönhammer. Functional renormalization group approach to correlated fermion systems. *Rev. Mod. Phys.*, 84:299–352, 2012.

[2] Peter Kopietz, Lorenz Bartosch, and Florian Schütz. *Introduction to the Functional Renormalization Group*. Springer, Berlin, 2010.

[3] C. Platt, W. Hanke, and R. Thomale. Functional renormalization group for multi-orbital fermi surface instabilities. *Advances in Physics*, 62(4-6):453–562, 2013.

[4] R Hedden, V Meden, Th Pruschke, and K Schönhammer. A functional renormalization group approach to zero-dimensional interacting systems. *Journal of Physics: Condensed Matter*, 16(29):5279, 2004.

[5] C. Karrasch, T. Enss, and V. Meden. Functional renormalization group approach to transport through correlated quantum dots. *Phys. Rev. B*, 73:235337, 2006.

[6] C. Karrasch, R. Hedden, R. Peters, Th. Pruschke, K. Schönhammer, and V. Meden. A finite-frequency functional renormalization group approach to the single impurity Anderson model. *Journal of Physics: Condensed Matter*, 20(34):345205, 2008.

[7] Carsten Honerkamp, Daniel Rohe, Sabine Andergassen, and Tilman Enss. Interaction flow method for many-fermion systems. *Phys. Rev. B*, 70:235115, 2004.

[8] Michael Kinza, Jutta Ortloff, Johannes Bauer, and Carsten Honerkamp. Alternative functional renormalization group approach to the single impurity Anderson model. *Phys. Rev. B*, 87:035111, 2013.

[9] C. Taranto, S. Andergassen, J. Bauer, K. Held, A. Katanin, W. Metzner, G. Rohringer, and A. Toschi. From infinite to two dimensions through the functional renormalization group. *Phys. Rev. Lett.*, 112:196402, 2014.

[10] N. Wentzell, C. Taranto, A. Katanin, A. Toschi, and S. Andergassen. Correlated starting points for the functional renormalization group. *Phys. Rev. B*, 91:045120, Jan 2015.

[11] Simon Streib, Aldo Isidori, and Peter Kopietz. Solution of the Anderson impurity model via the functional renormalization group. *Phys. Rev. B*, 87:201107, 2013.

[12] Severin Jakobs, Volker Meden, and Herbert Schoeller. Nonequilibrium functional renormalization group for interacting quantum systems. *Phys. Rev. Lett.*, 99:150603, 2007.

[13] R. Gezzi, Th. Pruschke, and V. Meden. Functional renormalization group for nonequilibrium quantum many-body problems. *Phys. Rev. B*, 75:045324, 2007.

[14] Severin G. Jakobs, Mikhail Pletyukhov, and Herbert Schoeller. Nonequilibrium functional renormalization group with frequency-dependent vertex function: A study of the single-impurity Anderson model. *Phys. Rev. B*, 81:195109, 2010.

[15] C. Karrasch, M. Pletyukhov, L. Borda, and V. Meden. Functional renormalization group study of the interacting resonant level model in and out of equilibrium. *Phys. Rev. B*, 81:125122, 2010.

[16] D. Kennes, S. Jakobs, C. Karrasch, and V. Meden. Renormalization group approach to time-dependent transport through correlated quantum dots. *Phys. Rev. B*, 85:085113, 2012.

[17] Manfred Salmhofer, Carsten Honerkamp, Walter Metzner, and Oliver Lauscher. Renormalization group flows into phases with broken symmetry. *Progress of Theoretical Physics*, 112(6):943–970, 2004.

[18] R. Gersch, C. Honerkamp, and W. Metzner. Superconductivity in the attractive Hubbard model: functional renormalization group analysis. *New Journal of Physics*, 10(4):045003, 2008.

[19] Andreas Eberlein and Walter Metzner. Effective interactions and fluctuation effects in spin-singlet superfluids. *Phys. Rev. B*, 87:174523, 2013.

[20] Andreas Eberlein and Walter Metzner. Superconductivity in the two-dimensional t-t'-Hubbard model. *Phys. Rev. B*, 89:035126, 2014.

[21] Stefan A. Maier, Andreas Eberlein, and Carsten Honerkamp. Functional renormalization group for commensurate antiferromagnets: Beyond the mean-field picture. *Phys. Rev. B*, 90:035140, 2014.

[22] Holger Gies and Christof Wetterich. Renormalization flow of bound states. *Phys. Rev. D*, 65:065001, 2002.

[23] Tobias Baier, Eike Bick, and Christof Wetterich. Temperature dependence of antiferromagnetic order in the Hubbard model. *Phys. Rev. B*, 70:125111, 2004.

[24] S. Diehl, H. Gies, J. Pawlowski, and C. Wetterich. Flow equations for the BCS-BEC crossover. *Phys. Rev. A*, 76:021602, 2007.

[25] S. Friederich, H. Krahl, and C. Wetterich. Functional renormalization for spontaneous symmetry breaking in the Hubbard model. *Phys. Rev. B*, 83:155125, 2011.

[26] Michael C. Birse, Boris Krippa, Judith A. McGovern, and Niels R. Walet. Pairing in many-fermion systems: an exact renormalisation group treatment. *Physics Letters B*, 605(34):287 – 294, 2005.

[27] Florian Schütz and Peter Kopietz. Functional renormalization group with vacuum expectation values and spontaneous symmetry breaking. *Journal of Physics A: Mathematical and General*, 39(25):8205, 2006.

[28] C. Husemann and M. Salmhofer. Efficient parametrization of the vertex function, Ω–scheme, and the (t,t')–Hubbard model at van Hove filling. *Phys. Rev. B*, 79:195125, 2009.

[29] Kay-Uwe Giering and Manfred Salmhofer. Self-energy flows in the two-dimensional repulsive Hubbard model. *Phys. Rev. B*, 86:245122, 2012.

[30] A. Katanin. Fulfillment of Ward identities in the functional renormalization group approach. *Phys. Rev. B*, 70:115109, 2004.

[31] T. Enss. *Renormalization, Conservation Laws and Transport in Correlated Electron Systems.* PhD thesis, Universität Stuttgart, 2005.

[32] Gordon Baym and Leo P. Kadanoff. Conservation laws and correlation functions. *Phys. Rev.*, 124:287–299, 1961.

[33] Gordon Baym. Self-consistent approximations in many-body systems. *Phys. Rev.*, 127:1391–1401, 1962.

[34] Kambis Veschgini and Manfred Salmhofer. Schwinger-Dyson renormalization group. *Phys. Rev. B*, 88:155131, 2013.

[35] N. Dupuis. Renormalization group approach to interacting fermion systems in the two-particle-irreducible formalism. *The European Physical Journal B - Condensed Matter and Complex Systems*, 48(3):319–338, 2005.

[36] N. Dupuis. Nonperturbative renormalization-group approach to fermion systems in the two-particle-irreducible effective action formalism. *Phys. Rev. B*, 89:035113, 2014.

[37] C. Wetterich. Bosonic effective action for interacting fermions. *Phys. Rev. B*, 75:085102, 2007.

[38] T. Schäfer, G. Rohringer, O. Gunnarsson, S. Ciuchi, G. Sangiovanni, and A. Toschi. Divergent precursors of the Mott-Hubbard transition at the two-particle level. *Phys. Rev. Lett.*, 110:246405, 2013.

[39] V. Janiš and V. Pokorný. Critical metal-insulator transition and divergence in a two-particle irreducible vertex in disordered and interacting electron systems. *Phys. Rev. B*, 90:045143,

2014.

[40] K.I. Aoki, A. Horikoshi, M. Taniguchi, and H. Terao. Non-perturbative renormalization group analysis in quantum mechanics. *Progress of Theoretical Physics*, 108(3):571–590, 2002.

[41] H. Gies. Introduction to the Functional RG and Applications to Gauge Theories. In J. Polonyi and A. Schwenk, editors, *Lecture Notes in Physics, Berlin Springer Verlag*, volume 852 of *Lecture Notes in Physics, Berlin Springer Verlag*, page 287, 2012.

[42] Michael Weyrauch. Functional renormalization group and quantum tunnelling. *Journal of Physics A: Mathematical and General*, 39(3):649, 2006.

[43] S. Nagy and K. Sailer. Functional renormalization group for quantized anharmonic oscillator. *Annals of Physics*, 326(8):1839 – 1876, 2011.

[44] J. Polonyi and K. Sailer. Effective action and density-functional theory. *Phys. Rev. B*, 66:155113, 2002.

[45] A. Schwenk and J. Polonyi. Towards Density Functional Calculations from Nuclear Forces. *arXiv:nucl-th/0403011*, 2004.

[46] Sandra Kemler and Jens Braun. Towards a renormalization group approach to density functional theory - general formalism and case studies. *Journal of Physics G: Nuclear and Particle Physics*, 40(8):085105, 2013.

[47] John W. Negele and Henri Orland. *Quantum many-particle systems.* Addison-Wesley, 1988.

[48] Jan M. Pawlowski. Aspects of the functional renormalisation group. *Annals of Physics*, 322(12):2831 – 2915, 2007.

[49] Severin G Jakobs, Mikhail Pletyukhov, and Herbert Schoeller. Properties of multi-particle Green's and vertex functions within Keldysh formalism. *Journal of Physics A: Mathematical and Theoretical*, 43(10):103001, 2010.

[50] Florian Schütz, Lorenz Bartosch, and Peter Kopietz. Collective fields in the functional renormalization group for fermions, Ward identities, and the exact solution of the Tomonaga-Luttinger model. *Phys. Rev. B*, 72:035107, 2005.

[51] J. White. Self-consistent Green functions for the Anderson impurity model. *Phys. Rev. B*, 45:1100–1106, 1992.

[52] Jens Braun. Fermion interactions and universal behavior in strongly interacting theories. *Journal of Physics G: Nuclear and Particle Physics*, 39(3):033001, 2012.

[53] R.M. Dreizler and E.K.U. Gross. *Density functional theory.* Springer, Berlin, 1990.